Chapter 3

Structure of Magnetic Fields

Many of the most interesting plasmas are permeated by or imbedded in magnetic fields.[1] As shown in Fig. 3.1, the magnetic field structures in which plasmas are immersed are very diverse; they can also be quite complicated. Many properties of magnetic fields in plasmas can be discussed without specifying a model for the plasma. This chapter discusses the plasma-independent, general properties ("kinematics") of magnetic fields, the models commonly used to describe them in plasma physics, and the coordinate systems based on them.

As indicated in Fig. 3.1, the generic structure of the magnetic field can be open (a–c and f) or closed (d,e). In open configurations the ends of the magnetic field lines[2] may intersect material boundaries (e.g., the earth in b), or be left unspecified (e.g., in a, on the field lines in b that do not intersect the earth, and in f). The magnetic field structure in closed configurations (d,e) is toroidal in character or topology. That is, its magnetic field lines are topologically equivalent (at least approximately) to lines on the surface of a torus or donut.

In most magnetized plasma situations the magnetic field has a nonzero value and a locally specified direction throughout the plasma. Also, the flow of magnetic field lines penetrating a closed surface in the plasma often[3] forms a bundle

[1] In plasma physics when we say "magnetic field" we usually mean magnetic induction field $\mathbf{B}$ — both because for many plasmas embedded in magnetic fields the plasma-induced currents are small and hence the magnetic permeability is approximately that of free space (i.e., $\mu \simeq \mu_0$), and because most plasma calculations, which use the microscopic Maxwell's equations, assume that the charged particles in the plasma produce currents in free space rather than doing so in a dielectric medium.

[2] While magnetic "field lines" or "lines of force" do not in fact exist (at least in the sense that they can be directly measured), they are very useful theoretical constructs for visualizing magnetic fields.

[3] However, closed magnetic flux surfaces do not exist in regions where the field lines are chaotic. Also, there are sometimes null points of the magnetic field within the plasma — for example in the neutral sheet in the earth's magnetosphere shown in Fig. 3.1b and along the axis in the wiggler field for the free electron laser shown in Fig. 3.1f. In addition, certain

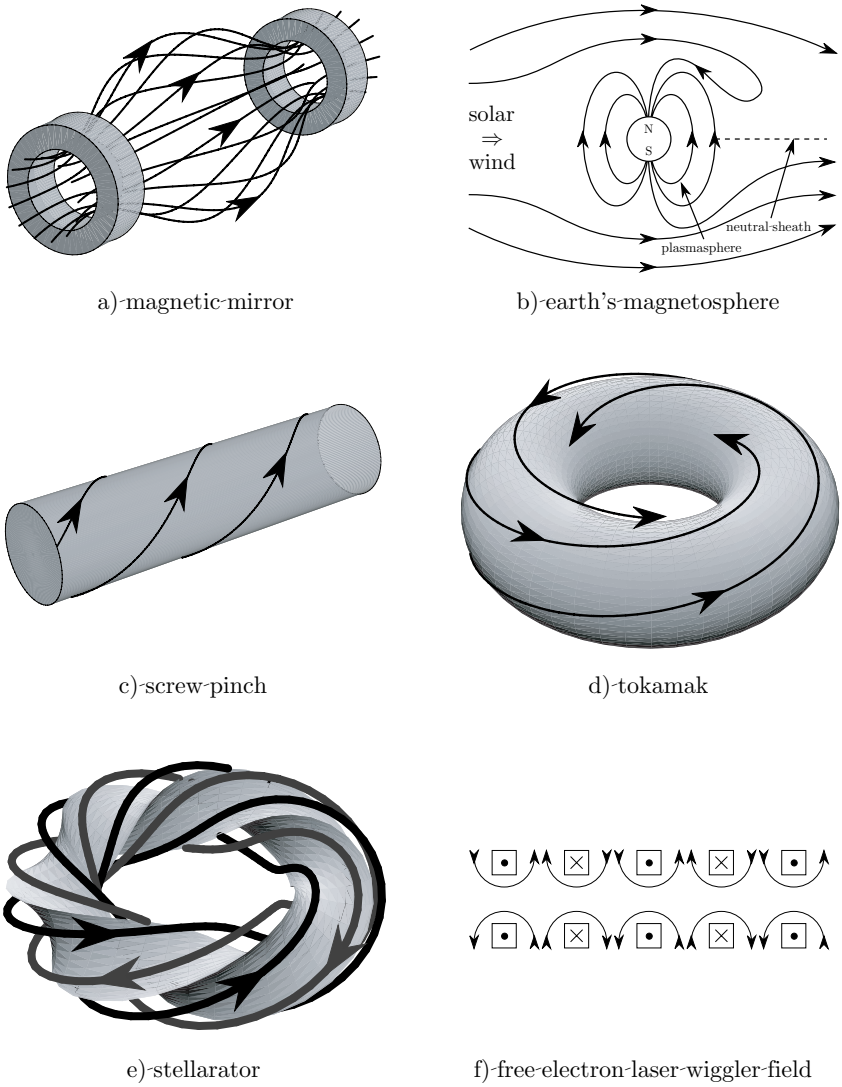

a)-magnetic-mirror b)-earth's-magnetosphere

c)-screw-pinch d)-tokamak

e)-stellarator f)-free-electron-laser-wiggler-field

Figure 3.1: Examples of magnetic field configurations in which plasmas are imbedded.

of magnetic field lines bounded by a *magnetic flux surface* within the magnetic

components of the magnetic field may have null points as well — for example the projection of the magnetic field in a screw pinch tokamak or stellarator in Figs. 3.1c–e along the helical pitch of a given magnetic field line.

configuration. When nested magnetic flux surfaces exist, they usually provide the most natural magnetic-field-based coordinate system because most plasma processes (charged particle motion, flows, transport) are much more rapid along magnetic field lines and within flux surfaces than across them.

The key magnetic field variations are evident in the magnetic field configurations illustrated in Fig. 3.1. Namely, while magnetic field lines point in a given direction at any specified point, they can curve and twist, and their density can vary in space. The general properties of curves along a vector field such as the magnetic field are summarized in Section D.6.

The first section of this chapter introduces simple models (quadratic and sinusoidal magnetic well, and sheared slab magnetic field) that include the four most important local magnetic field properties for plasma physics (namely, parallel and perpendicular gradients, curvature and shear). These simple models will be used to explore the most fundamental effects of magnetic fields in many areas of plasma physics throughout the remainder of this book. The second section introduces the global magnetic field representations and magnetic-field-based coordinate systems that are used in modeling plasma processes on (longer) time scales where charged particles travel significant distances along magnetic fields. While the magnetic fields in which plasmas are imbedded are seldom straight in Cartesian coordinates, one can develop coordinate systems in which the magnetic field lines are straight. Such coordinates greatly facilitate analyses of magnetized plasmas. The third section develops the basic ideas of magnetic island structures that can form in the sheared slab model when a resonant perturbation is added. The next three sections discuss the simplest forms and properties of magnetic field coordinate systems for open (Section 3.4) and closed (Sections 3.5, 3.6) magnetic field systems. Finally, Section 3.7 gives the general forms of all the local differential propoerties of the vector magnetic field — gradients, divergence, curvature, shear and torsion, and the general expansion of the magnetic field $\mathbf{B}$ in terms of them.

3.1 Local Properties

The SI (mks) units for the magnetic field strength are webers/m^2; thus, we can think of the magnetic field strength as representing the number of magnetic field lines (webers) per unit area (m^2). Typically, the magnetic field strength varies as we move along a magnetic field line. We can distinguish the effects of variations in the magnetic field strength from the effects of changes in its direction by representing the magnetic field as

$$\mathbf{B} \,=\, B(\mathbf{x})\,\hat{\mathbf{b}}, \quad \text{with } \hat{\mathbf{b}} \,\equiv\, \mathbf{B}/B, \tag{3.1}$$

in which $B \equiv |\mathbf{B}| \equiv \sqrt{\mathbf{B}\cdot\mathbf{B}}$ is the magnetic field strength and $\hat{\mathbf{b}}$ is the local unit vector along $\mathbf{B}$, both at the point $\mathbf{x}$. Since there are no magnetic monopoles in nature, a magnetic field must be divergence free. (Such a vector field is called a solenoidal field.) Thus, using the representation of $\mathbf{B}$ given in (3.1) and the

vector identity (**??**), we must have

$$0 = \boldsymbol{\nabla}\cdot\mathbf{B} = \hat{\mathbf{b}}\cdot\boldsymbol{\nabla}B(\ell) + B\,\boldsymbol{\nabla}\cdot\hat{\mathbf{b}}. \tag{3.2}$$

An equation governing the variation of the magnetic field strength B along any field line can be determined by rearranging this equation to yield

$$\frac{\partial B}{\partial \ell} \equiv \hat{\mathbf{b}}\cdot\boldsymbol{\nabla}B = -B\,\boldsymbol{\nabla}\cdot\hat{\mathbf{b}}, \tag{3.3}$$

in which ℓ is the distance along a magnetic field line. Hence, if the magnetic field strength (number of field lines per unit area) is increasing ($\partial B/\partial\ell > 0$) as one moves along a magnetic field line, the local unit vectors along magnetic field lines must be converging ($\boldsymbol{\nabla}\cdot\hat{\mathbf{b}} < 0$); conversely, for a decreasing magnetic field strength ($\partial B/\partial\ell < 0$) the field line unit vectors diverge ($\boldsymbol{\nabla}\cdot\hat{\mathbf{b}} > 0$).

We will often be interested in describing mathematically the parallel ($\|$) variation of the magnetic field strength B. Near a minimum in the magnetic field strength along a magnetic field line the field strength B can be represented by a quadratic approximation:

$$\boxed{B_{\rm qw} = B_{\rm min}\left(1+\frac{\ell^2}{L_\|^2}\right), \quad \text{quadratic well (qw) model,}} \tag{3.4}$$

in which at $B = B_{\rm min}$ where $\ell = 0$ we have $\partial B/\partial\ell|_{\ell=0} = 0$ and $\partial^2 B/\partial\,\ell^2|_{\ell=0} > 0$, and by definition

$$L_\| \equiv \sqrt{\frac{2\,B}{\partial^2 B/\partial\ell^2}\bigg|_{B=B_{\rm min}}}\,. \tag{3.5}$$

The characteristic scale length $L_\|$ is the parallel distance over which the magnetic field strength doubles — in this lowest order approximation.

The magnetic field strength often varies sinusoidally along a magnetic field line. A convenient model for this variation is

$$\begin{aligned}\boxed{B_{\rm sin}(\ell) = B_{\rm min} + \left(\frac{B_{\rm max}-B_{\rm min}}{2}\right)\left[1-\cos\left(\frac{2\pi\ell}{L_\ell}\right)\right]} \\ = B_{\rm min} + \Delta B\,\sin^2\frac{\pi\ell}{L_\ell}, \quad \text{sinusoidal (sin) model.}\end{aligned} \tag{3.6}$$

Here, $B_{\rm max}$ is the maximum field strength along a field line which occurs at $\ell = \pm L_\ell/2$ in this model, and $\Delta B \equiv B_{\rm max} - B_{\rm min}$ is the amplitude of the variation of B along a field line within the periodicity length L_ℓ. The ℓ variation of $B_{\rm sin}$ near its minimum can be represented by the parabolic well model in (3.4) with $L_\| = (B_{\rm min}/\Delta B)^{1/2}L_\ell/\pi$. The ratio of the maximum to minimum magnetic field strength along a field line is:

$$\boxed{R_m \equiv \frac{B_{\rm max}}{B_{\rm min}} = 1 + \frac{\Delta B}{B_{\rm min}}, \quad \text{magnetic mirror ratio.}} \tag{3.7}$$

Mirror ratios range from values of order 2 to 10 or more for typical magnetic mirrors (Fig. 3.1a) and the earth's magnetosphere (Fig. 3.1b), to only slightly greater than unity in toroidal devices (Fig. 3.1d,e) where the magnetic field strength varies only slightly as we move along the helical magnetic field lines from the outside to the inside of the torus. Note from (3.3) that at an extremum (minimum or maximum) of the magnetic field strength where $\partial B/\partial \ell = 0$ the local unit vectors along field lines are divergence-free — they neither converge nor diverge.

The magnetic field can also vary — both in magnitude and direction — in directions perpendicular (transverse) to the magnetic field direction. The sheared slab model, which we now discuss, approximates the local perpendicular variations of typical magnetic field structures that are most important in plasma physics. In it a local Cartesian coordinate system is constructed at a given point. The z axis is taken to be along the magnetic field at the point where a magnetic field line passes through the origin of the coordinate system. The x axis is taken to be in the "radial" (across flux surface) direction in which the most significant variations (in plasma parameters and in the density of magnetic field lines) occur in the plane perpendicular to the magnetic field. The y axis is taken to be in the azimuthal (or within flux surface) direction of least variation; i.e., it is the "ignorable" coordinate, at least approximately. For example, for a cylindrical magnetized plasma we anticipate mainly a radial variation in the plasma parameters: for this case the sheared slab model x, y, z coordinates would correspond to $r - r_0, r_0\theta$ and z where $r = r_0$ is the cylindrical radius of the magnetic field line that passes through the origin of the sheared slab model. The word slab in the title of the model indicates that only a thin "radial" (x) slice of the magnetic configuration is being considered.

A local expansion of the magnetic field that captures its most important perpendicular variations is

$$\boxed{\mathbf{B}_{\rm ss} \;=\; B_0 \left[\left(1 + \frac{x}{L_B} \right) \hat{\mathbf{e}}_{\rm z} + \frac{z}{R_C}\, \hat{\mathbf{e}}_{\rm x} + \frac{x}{L_S}\, \hat{\mathbf{e}}_{\rm y} \right], \quad \text{sheared slab (ss) model,}} \tag{3.8}$$

in which B_0 is the strength of the magnetic field (or density of magnetic field lines) at the origin where $\mathbf{x} \equiv (x, y, z) = (0, 0, 0)$. Here, as indicated in Fig. 3.2, the $\hat{\mathbf{e}}_{\rm z}$ term represents the lowest order magnetic field (the unity) and the perpendicular spatial gradient of its magnitude ($1/L_B$), the $\hat{\mathbf{e}}_{\rm x}$ term represents the magnetic field curvature ($1/R_C$), and the $\hat{\mathbf{e}}_{\rm y}$ term represents the differential twisting (shear, $1/L_S$) of the magnetic field lines. These fundamental magnetic field properties will be explained and defined more precisely below and in the following sections. [Torsion (uniform twisting — see Section 3.7 below and D.6) of magnetic field lines such as in a uniform helical twist of the field lines in the screw pinch shown in Fig. 3.1c is not included in the sheared slab model because the $\hat{\mathbf{e}}_{\rm z}$ vector is taken to be in a locally fixed rather than rotating direction.] Since the model represents a Taylor series expansion of the magnetic field about a given point, it is only valid for small distances from the origin — $|x/L_B| << 1$,

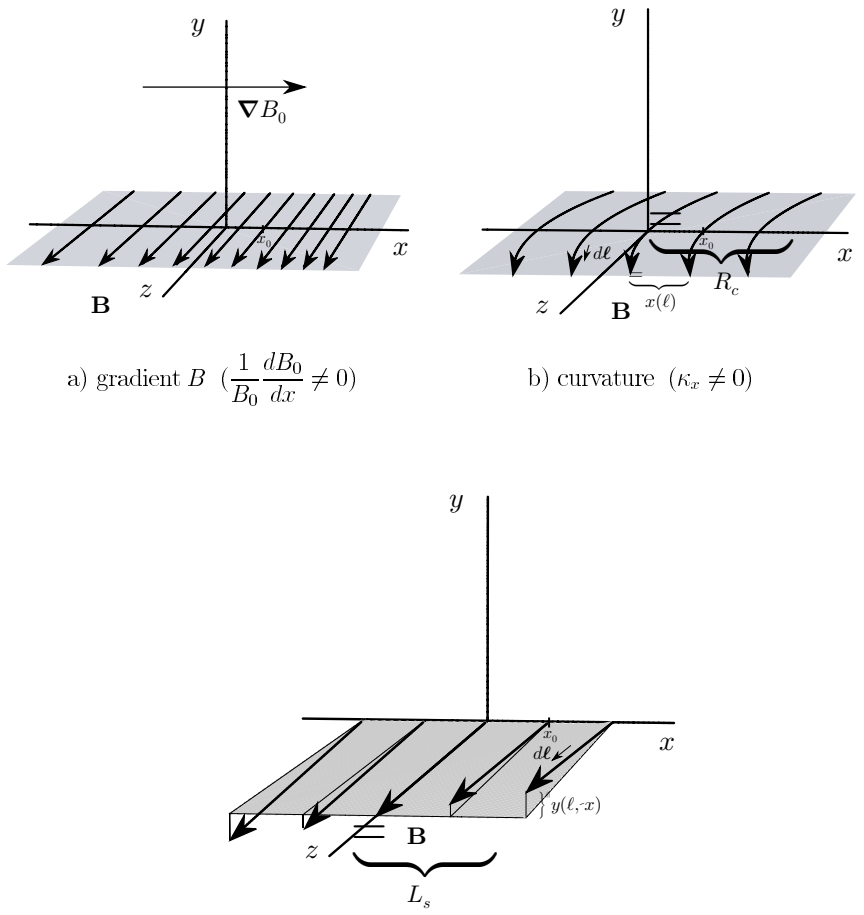

Figure 3.2: Magnetic field line characteristics included in the sheared slab magnetic field model. Each sketch indicates the behavior of magnetic field lines when only the indicated coefficient does not vanish.

$|z/R_C| << 1$, $|x/L_S| << 1$.

Calculating the magnitude of the magnetic field using $B \equiv |\mathbf{B}| = \sqrt{\mathbf{B}\cdot\mathbf{B}}$, we find, to lowest order in the distance from the origin,

$$B_{\rm ss} \equiv |\mathbf{B}_{\rm ss}| = B_0\left(1 + \frac{x}{L_B} + \mathcal{O}\left\{\frac{x^2}{L_B^2}, \frac{x^2}{L_S^2}, \frac{z^2}{R_C^2}\right\}\right) \simeq B_0\left(1 + \frac{x}{L_B}\right). \quad (3.9)$$

Thus, we identify

$$\boxed{L_B \equiv \frac{B}{dB/dx} = \left(\frac{d\ln B}{dx}\right)^{-1}, \quad \text{perpendicular } \boldsymbol{\nabla} B \text{ scale length,}} \tag{3.10}$$

in which the differential is to be evaluated at the origin of our local Cartesian coordinate system. The gradient scale length L_B is the radial (x) distance over which the magnitude of the magnetic field would double in this linear model. Hence, the $1/L_B$ term in (3.8) represents the gradient in the magnetic field strength (density of magnetic field lines) in the x direction (cf., Fig. 3.2c). Henceforth, we will call this the perpendicular $\boldsymbol{\nabla} B$ or gradient B term.

The curvature of a magnetic field line can be determined as follows. First, we propose that a coordinate function $x(\ell)$ represents the x variation of a magnetic field line as we move a distance ℓ along it. Then, the x component of the curvature of the magnetic field line is defined as the second derivative of $x(\ell)$ along the field line:

$$\text{curvature} \equiv \frac{d^2x(\ell)}{d\ell^2}. \tag{3.11}$$

For a magnetic field line near the origin of the sheared slab model coordinate system, by geometry we have

$$\frac{dx(\ell)}{d\ell} \simeq \frac{B_x(\ell)}{B} \simeq \frac{B_x(z)}{B_0} = \frac{z}{R_C} \tag{3.12}$$

and hence

$$\text{curvature} \equiv \frac{d^2x}{d\ell^2} \simeq \frac{d}{dz}\left[\frac{B_x(z)}{B_0}\right] = \frac{1}{R_C} \tag{3.13}$$

in which $B_x \equiv \hat{\mathbf{e}}_\mathbf{x} \cdot \mathbf{B}$ is the x component of the vector magnetic field. The radius of curvature R_C of the magnetic field in the sheared slab model is the radius of the circle that is tangent to and has the same curvature as the magnetic field line that passes through the origin. Integrating (3.12) a short distance ($|z/R_C| << 1$) along the field line that passes through $\mathbf{x} = (x_0, 0, 0)$ yields an equation for the field lines' trajectory (cf., Fig. 3.2a) in the x–z plane (to lowest order $d\ell \simeq dz$ and $\ell \simeq z$ near the origin):

$$x = x_0 + z^2/2R_C, \quad \text{for } y = \text{constant}, \tag{3.14}$$

which again shows that $1/R_C$ measures the curvature of the field line.

The formal definition of the curvature vector $\boldsymbol{\kappa}$ for a vector magnetic field $\mathbf{B} \equiv B\hat{\mathbf{b}}$ is [see (**??**) in Section D.6]

$$\boxed{\boldsymbol{\kappa} \equiv \frac{d^2\mathbf{x}}{d\ell^2} = (\hat{\mathbf{b}} \cdot \boldsymbol{\nabla})\hat{\mathbf{b}} = -\frac{\mathbf{R}_C}{R_C^2}, \quad \mathbf{B} \text{ field curvature vector.}} \tag{3.15}$$

Evaluating this expression for the sheared slab model magnetic field in (3.8), we obtain (near the origin where $d\ell \simeq dz$ and $|x| << L_B$)

$$\boldsymbol{\kappa} \;=\; \frac{\partial \hat{\mathbf{b}}}{\partial \ell} \;\simeq\; \frac{\partial}{\partial z}\left[\hat{\mathbf{e}}_{\rm z} + \frac{(z/R_C)\,\hat{\mathbf{e}}_{\rm x} + (x/L_S)\,\hat{\mathbf{e}}_{\rm y}}{1 + x/L_B}\right] \;\simeq\; \frac{1}{R_C}\,\hat{\mathbf{e}}_{\rm x} \;\equiv\; \kappa_x \hat{\mathbf{e}}_{\rm x}. \qquad (3.16)$$

Thus, R_C is the inverse of the (normal, x direction) curvature of the magnetic field:

$$\boxed{R_C \;\equiv\; 1/|\kappa_x|, \quad \text{radius of curvature.}} \qquad (3.17)$$

Note that the absolute value is needed because vectorially the radius of curvature vector $\mathbf{R}_C$ points in the opposite direction from the curvature vector: $\boldsymbol{\kappa} = -\mathbf{R}_C/R_c^2$ — see Fig. **??** and Eq. (**??**) in Section D.6. Thus, for the sheared slab model the vectorial radius of curvature is $\mathbf{R}_C \equiv -\boldsymbol{\kappa}/|\boldsymbol{\kappa}|^2 = -R_C\hat{\mathbf{e}}_{\rm x}$, which points from the point $\mathbf{x} = (R_C, 0, 0)$ to the origin.

The magnetic field line curvature vector $\boldsymbol{\kappa}$ can in general be written in a more illustrative and useful form (for situations where currents flow in the plasma) using $\hat{\mathbf{b}} \equiv \mathbf{B}/B$ and the magnetostatic Ampere's law $\boldsymbol{\nabla}\times\mathbf{B} = \mu_0\mathbf{J}$:

$$\begin{aligned}\boldsymbol{\kappa} \;&\equiv\; (\hat{\mathbf{b}}\cdot\boldsymbol{\nabla})\hat{\mathbf{b}} \;=\; -\,\hat{\mathbf{b}}\times(\boldsymbol{\nabla}\times\hat{\mathbf{b}}) \;=\; -\,\hat{\mathbf{b}}\times(\boldsymbol{\nabla}\times\mathbf{B}/B) \\ &=\; -\,\hat{\mathbf{b}}\times[\boldsymbol{\nabla}(1/B)\times\mathbf{B}] - \hat{\mathbf{b}}\times(\boldsymbol{\nabla}\times\mathbf{B})/B \;=\; -\,\hat{\mathbf{b}}\times(\hat{\mathbf{b}}\times\boldsymbol{\nabla}\ln B) + \mu_0\mathbf{J}\times\mathbf{B}/B^2 \\ &=\; (1/B)[\boldsymbol{\nabla} - \hat{\mathbf{b}}(\hat{\mathbf{b}}\cdot\boldsymbol{\nabla})]B + \mu_0\mathbf{J}\times\mathbf{B}/B^2, \qquad (3.18)\end{aligned}$$

in which the vector identities (**??**), (**??**), and (**??**) have been used in successive steps. Defining

$$\boldsymbol{\nabla}_\perp \;\equiv\; \boldsymbol{\nabla} - \hat{\mathbf{b}}\,(\hat{\mathbf{b}}\cdot\boldsymbol{\nabla}) \;=\; -\,\hat{\mathbf{b}}\times(\hat{\mathbf{b}}\times\boldsymbol{\nabla}), \quad \text{gradient perpendicular to } \mathbf{B}, \qquad (3.19)$$

to represent the components of the gradient operator in directions perpendicular to the magnetic field $\mathbf{B}$, we can write the final form in (3.18) in general as

$$\boxed{\boldsymbol{\kappa} \;=\; \boldsymbol{\nabla}_\perp \ln B + \frac{\mu_0\mathbf{J}\times\mathbf{B}}{B^2}, \quad \text{relation of curvature to } \boldsymbol{\nabla}_\perp B \text{ and } \mathbf{J}.} \qquad (3.20)$$

Near the origin of the sheared slab model, the $\hat{\mathbf{e}}_{\rm x}$ component of this equation yields

$$\kappa_x \;\equiv\; \frac{1}{R_C} \;=\; \frac{1}{B}\frac{dB}{dx} + \frac{\mu_0 J_y}{B} \;=\; \frac{1}{L_B} + \frac{\mu_0 J_y}{B}. \qquad (3.21)$$

When there is no current in the $\hat{\mathbf{e}}_{\rm y}$ direction in the sheared slab model, we have $1/R_C = 1/L_B$.

The shear in a magnetic field can be understood as follows. A magnetic field line can rotate about the z axis because of torsion (twisting at a constant angular rate) and shear (differential twisting) — see Section D.6. As noted above, the sheared slab model does not include torsion. The shear in the magnetic field

can be defined for our Cartesian coordinate system through the x derivative of the $y(\ell)$ coordinate variation along a magnetic field line:

$$\text{shear} \equiv \frac{d}{dx}\left[\frac{dy(\ell)}{d\ell}\right]. \tag{3.22}$$

For a magnetic field line near the origin of the sheared slab model coordinate system, by geometry we have

$$\frac{dy(\ell)}{d\ell} \simeq \frac{B_y}{B_0} \simeq \frac{x}{L_S}.$$

Thus, in the sheared slab model we have

$$\boxed{\text{shear} \equiv \frac{d}{dx}\left(\frac{dy}{d\ell}\right) \simeq \frac{d}{dx}\left[\frac{B_y(x)}{B_0}\right] \simeq \frac{1}{L_S}.} \tag{3.23}$$

The shear length L_S is the linear extrapolation distance in the x direction over which the magnetic field would differentially twist through an angle of one radian (i.e., to where $B_y = B_0$). Integrating (3.22) a short distance ($|z/L_S| << 1$) along the field line that passes through the point $\mathbf{x} = (x, y_0, 0)$ yields an equation for its trajectory (cf., Fig. 3.2b) in the y–z plane:

$$y = y_0 + x\, z/L_S, \quad \text{for } x = \text{constant}, \tag{3.24}$$

which shows that $1/L_S$ measures the differential twisting of the field lines out of the the x–z plane and hence the shear in the magnetic field lines.

The formal definition of the local shear ς in a vector field $\mathbf{B} \equiv B\hat{\mathbf{b}}$ is [see (3.151) below and (**??**) in Section D.6]

$$\boxed{\varsigma \equiv \frac{(\hat{\mathbf{b}}\times\boldsymbol{\nabla}\psi)\cdot\boldsymbol{\nabla}\times(\hat{\mathbf{b}}\times\boldsymbol{\nabla}\psi)}{|\hat{\mathbf{b}}\times\boldsymbol{\nabla}\psi|^2} = \frac{(\mathbf{B}\times\boldsymbol{\nabla}\psi)\cdot\boldsymbol{\nabla}\times(\mathbf{B}\times\boldsymbol{\nabla}\psi)}{B^2|\boldsymbol{\nabla}\psi|^2}, \quad \text{local shear}} \tag{3.25}$$

in which $\boldsymbol{\nabla}\psi$ is the gradient of an assumed magnetic flux function ψ and for the last form we have used (3.1) and vector identities (**??**), (**??**) and (**??**). For our sheared slab model $\psi \to x$, $\boldsymbol{\nabla}\psi \to \boldsymbol{\nabla}x = \hat{\mathbf{e}}_{\rm x}$ and thus $\hat{\mathbf{b}}\times\boldsymbol{\nabla}\psi \to \hat{\mathbf{b}}\times\hat{\mathbf{e}}_{\rm x} = \hat{\mathbf{e}}_{\rm y} - \hat{\mathbf{e}}_{\rm z}(x/L_S)/(1+x/L_B)$. Note that near the origin of the sheared slab model geometry $|\hat{\mathbf{b}}| \simeq 1$ and $|\hat{\mathbf{b}}\times\boldsymbol{\nabla}\psi| \simeq 1$. Thus, evaluating the shear definition in (3.25) for the sheared slab model we obtain

$$\varsigma \simeq \hat{\mathbf{e}}_{\rm y}\cdot\boldsymbol{\nabla}\times(\hat{\mathbf{b}}\times\hat{\mathbf{e}}_{\rm x}) \simeq 1/L_S. \tag{3.26}$$

By construction, the magnetic field in the sheared slab model satisfies the solenoidal or no magnetic monopole condition for a magnetic induction field, i.e., $\boldsymbol{\nabla}\cdot\mathbf{B}_{\rm ss} = 0$. However, its curl (rotation) does not vanish:

$$\boldsymbol{\nabla}\times\mathbf{B}_{\rm ss} = B_0\left[\left(\frac{1}{R_C} - \frac{1}{L_B}\right)\hat{\mathbf{e}}_{\rm y} + \frac{1}{L_S}\,\hat{\mathbf{e}}_{\rm z}\right]. \tag{3.27}$$

In equilibrium situations where the magnetostatic Ampere's law $\boldsymbol{\nabla}\times\mathbf{B} = \mu_0\mathbf{J}$ applies, the full generality of the sheared slab model is appropriate only if electrical currents flow in the plasma. For vacuum or very low plasma pressure situations where no significant currents flow in a magnetized plasma, we must have $1/R_C = 1/L_B$ and $1/L_S = 0$. The curvature $(1/R_C)$ can deviate from the inverse gradient length $(1/L_B)$ only if electrical current flows in the y direction, as indicated by both (3.21) and (3.27). Since for strong magnetic fields it is harder for charged particles and hence plasma currents to flow across magnetic fields compared to along them, the y component of the current is typically small and usually $1/R_C \simeq 1/L_B$. Magnetic shear $(1/L_S)$ is possible (in this torsion-free model) only if current flows in the z (magnetic field) direction. These points will be made more quantitatively explicit in Sections 3.7, 5.3 and 20.1.

The parallel quadratic well, sinusoidal and sheared slab models represent the most important spatial variations of the magnetic field around a given point. Any given physical situation can be modeled with these models by specifying the characteristic scale lengths for the local properties of the magnetic field: parallel gradient B scale lengths $L_\parallel$ and L_ℓ, perpendicular gradient B length L_B, curvature radius R_C and shear length L_S. While these models provide suitable lowest order "local" descriptions for most magnetized plasma situations, they are not the most general magnetic field descriptions. In particular, they do not allow for torsion or all the possible magnetic field variations in the y and z directions. The most general local expansion of a magnetic field is discussed in Section 3.7. Also, the local expansions do not in general provide global (i.e., valid over all space) descriptions of the magnetic field. The remaining sections of this chapter develop more complete, but correspondingly more complex, magnetic field models.

3.2 Magnetic Field Representations and Coordinate Systems

In the preceding section we developed local Taylor series expansions of a magnetic field $\mathbf{B}$ about a given point. While these expansions are very useful for understanding the local differential properties (gradients, curvature, shear) of a magnetic field, in general they do not provide a global description of it. Charged particles in plasmas move over long distances along magnetic field lines for most time scales of interest. Also, they typically move much more rapidly along magnetic field lines than perpendicular to them; this causes the properties of a magnetized plasma to be very anisotropic relative to the magnetic field direction. In order to develop compact descriptions of magnetized plasmas it is most convenient to use coordinate systems based on the global structure of the magnetic field — so-called magnetic field line or magnetic flux coordinate systems. Magnetic flux coordinates are curvilinear coordinates that are chosen so that the equation of a magnetic field line is a straight line in the chosen coordinates. They are the most useful coordinates because they facilitate separation

of plasma effects along and perpendicular to magnetic field lines. This section discusses calculations of magnetic field lines, and magnetic field representations and coordinate systems that describe the entire magnetic field structure.

The global structure of the magnetic field can in principle be obtained by simply integrating the differential equations of a curve that follows a magnetic field line. Defining $\mathbf{x}(\ell)$ to be the trajectory along a magnetic field line, the vector $d\mathbf{x}(\ell)/d\ell$ that is locally tangent to the magnetic field is given by

$$\boxed{\left.\frac{d\mathbf{x}(\ell)}{d\ell}\right|_{\text{along } \mathbf{B}} = \frac{\mathbf{B}}{B} = \hat{\mathbf{b}}, \quad \text{field line equation.}} \tag{3.28}$$

This is the fundamental definition of a magnetic field line that we will use throughout the remainder of this book. Taking the $\hat{\mathbf{e}}_{\mathrm{x}}$, $\hat{\mathbf{e}}_{\mathrm{y}}$, and $\hat{\mathbf{e}}_{\mathrm{z}}$ projections of this fundamental field line definition, we obtain

$$\frac{dx}{B_x} = \frac{dy}{B_y} = \frac{dz}{B_z} = \frac{d\ell}{B}. \tag{3.29}$$

Note that these field line differential equations can also be obtained from the condition that a vector differential length $d\boldsymbol{\ell}$ along the magnetic field $\mathbf{B}$ must be parallel to it: $d\boldsymbol{\ell}\times\mathbf{B} = \mathbf{0}$.

For simple magnetic field systems we can directly integrate the three independent equations in (3.29) to obtain a mathematical description of the magnetic field. For example, we performed such integrations for the sheared slab model in the special cases of no shear and little perpendicular gradient B or curvature — see (3.14) and (3.24). For such systems the constants of integration provide labels for the magnetic field lines — x_0 and y_0 for the two special sheared slab model cases. However, it is often impractical or impossible to obtain a global magnetic field description by directly integrating the equations that describe a magnetic field line trajectory. For example, integrating the three equations for the complete sheared slab model in (3.8) results in a set of three interrelated, implicit equations for which a closed solution is not possible, except in the vicinity of the origin (see Problem 3.7).

For a magnetic field in free space (i.e., in a vacuum), or in the limit where the currents flowing in the plasma are negligible, the equilibrium Ampere's law becomes simply $\boldsymbol{\nabla}\times\mathbf{B} = \mathbf{0}$. This equation can be satisfied by writing the magnetic field in terms of a scalar potential Φ_M:

$$\mathbf{B} = -\boldsymbol{\nabla}\Phi_M, \quad \text{vacuum magnetic field representation.} \tag{3.30}$$

For this case the solenoidal (no magnetic monopoles) condition $\boldsymbol{\nabla}\cdot\mathbf{B} = 0$ becomes the Laplace equation

$$\nabla^2\Phi_M = 0. \tag{3.31}$$

Methods for solving the Laplace equation in various geometries are available in many books on electromagnetic theory and other areas of physics. For magnetized plasmas such solutions are useful mainly in vacuum regions outside the

plasma, or as the lowest order magnetic field structure for cases where currents in the plasma do not significantly change the magnetic field. However, for many important magnetized plasma situations the electrical currents flowing in the plasma are significant, and in fact very important, in determining the structure and even topology of the magnetic field. Thus, solutions of (3.31) for vacuum magnetic fields are not always useful for magnetized plasmas and we must look elsewhere for broadly applicable descriptions.

Like any vector field subject to the solenoidal condition ($\boldsymbol{\nabla}\cdot\mathbf{B} = 0$), the magnetic induction field $\mathbf{B}$ can be written in terms of a vector potential $\mathbf{A}$:

$$\mathbf{B} = \boldsymbol{\nabla}\times\mathbf{A}. \tag{3.32}$$

For example, an appropriate vector potential for the sheared slab model is

$$\mathbf{A}_{\rm ss} = B_0\left(x + \frac{x^2}{2L_B} - \frac{z^2}{2R_C}\right)\hat{\mathbf{e}}_{\rm y} - B_0\frac{x^2}{2L_S}\,\hat{\mathbf{e}}_{\rm z}, \tag{3.33}$$

as can be verified by substituting it into (3.32) and comparing the result to (3.8).

Alternatively (see Section D.5), the magnetic field can be written as

$$\boxed{\mathbf{B} = \boldsymbol{\nabla}\alpha\times\boldsymbol{\nabla}\beta, \quad \text{Clebsch representation,}} \tag{3.34}$$

in which $\alpha(\mathbf{x})$ and $\beta(\mathbf{x})$ are scalar stream functions (i.e., functions that are constant along the vector field $\mathbf{B}$) since $\mathbf{B}\cdot\boldsymbol{\nabla}\alpha = \mathbf{B}\cdot\boldsymbol{\nabla}\beta = 0$. Note that the representations of $\mathbf{B}$ in (3.32) and (3.34) are equivalent if we define

$$\mathbf{A} = \alpha\boldsymbol{\nabla}\beta, \quad \text{or} \quad \mathbf{A} = -\beta\boldsymbol{\nabla}\alpha, \tag{3.35}$$

since using vector identities (**??**), (**??**), and (**??**), we have $\boldsymbol{\nabla}\times\alpha\boldsymbol{\nabla}\beta = \boldsymbol{\nabla}\alpha\times\boldsymbol{\nabla}\beta$ and $-\boldsymbol{\nabla}\times\beta\boldsymbol{\nabla}\alpha = -\boldsymbol{\nabla}\beta\times\boldsymbol{\nabla}\alpha = \boldsymbol{\nabla}\alpha\times\boldsymbol{\nabla}\beta$. Note also that the vector potential $\mathbf{A}$ and the stream functions α, β are somewhat arbitrary since they yield the same magnetic induction field $\mathbf{B}$ under the gauge transformations $\mathbf{A} \to \mathbf{A} + \boldsymbol{\nabla}\chi(\mathbf{x})$, and $\alpha \to \alpha + f_1(\beta)$ or $\beta \to \beta + f_2(\alpha)$ (but not both f_1, f_2 simultaneously) in which χ, f_1, and f_2 are arbitrary scalar functions of the variables indicated. While the stream functions α, β must be continuous, they can be multivalued (e.g., they can involve angular or cyclic variables). For examples of α and β stream functions, see Problem 3.7, which develops them for the sheared slab model, and the following sections.

The Clebsch representation of the magnetic field can be used as a basis for a coordinate system that represents the global magnetic field structure — the Clebsch magnetic coordinate system. Along magnetic field lines, which follow the curve given by (3.28), we have $d\alpha/d\ell = (d\mathbf{x}/d\ell)\cdot\boldsymbol{\nabla}\alpha = (\mathbf{B}\cdot\boldsymbol{\nabla}\alpha)/B = 0$ and similarly $d\beta/d\ell = 0$. Thus, magnetic field lines lie within $\alpha(\mathbf{x}) =$ constant and $\beta(\mathbf{x}) =$ constant surfaces. Further, since $\boldsymbol{\nabla}\alpha\times\boldsymbol{\nabla}\beta$ points in the direction of (and is equal to) $\mathbf{B}$, the intersection of the α, β surfaces defines a given magnetic field line. Hence, α and β are labels for a particular magnetic field line.

Because the α, β stream functions label magnetic field lines in the plane perpendicular to $\mathbf{B}$, they can provide curvilinear coordinates perpendicular to the magnetic field. There is no obvious choice for the coordinate along the magnetic field. From physical considerations it is convenient to choose the length ℓ (measured from some suitable surface) along field lines. [However, other coordinates along the magnetic field are often used, e.g., $d\Phi_M = -Bd\ell$ for the vacuum magnetic field in (3.30)]. Unfortunately, the α, β, ℓ coordinates are in general not orthogonal and not available in closed form solutions. These complications plus their possible multivaluedness make them an awkward choice as the basis for a magnetic-field-based coordinate system. However, because of their simplicity and generality they are often useful for proofs concerning equilibrium, stability and transport properties of magnetized plasmas.

Magnetic flux surfaces usually provide a better basis for developing magnetic-field-based coordinate systems for plasma physics. The magnetic flux Ψ through a surface S encompassed by a closed curve C is in general defined by

$$\boxed{\Psi \;=\; \iint_S d\mathbf{S}\cdot\mathbf{B} \;=\; \iint_S d\mathbf{S}\cdot\boldsymbol{\nabla}\times\mathbf{A} \;=\; \oint_C d\boldsymbol{\ell}\cdot\mathbf{A}, \quad \text{magnetic flux,}} \tag{3.36}$$

in which we have used Stokes' theorem (**??**) in the last step. In this book we will use a capital letter Ψ to indicate the total magnetic flux in its normal units (webers), and a small Greek letter ψ to indicate a magnetic flux component that has been normalized in some way (e.g., often $\psi = \Psi/2\pi$). Since magnetic flux surfaces encompass the bundle of magnetic field lines within the surface S, they must satisfy

$$\boxed{\mathbf{B}\cdot\boldsymbol{\nabla}\Psi \;=\; 0, \quad \text{magnetic flux surface condition.}} \tag{3.37}$$

Thus, $\boldsymbol{\nabla}\Psi$, which by definition [see (**??**)] is normal to the flux surface $\Psi(\mathbf{x})$, is orthogonal to the magnetic field $\mathbf{B}$ and hence to its field lines. That is, magnetic field lines lie within $\Psi(\mathbf{x}) =$ constant surfaces.

For a Clebsch coordinate system with $\mathbf{A} = \alpha\boldsymbol{\nabla}\beta$ and a closed contour C_β, the magnetic flux becomes

$$\Psi_\wedge \;=\; \iint_{S_\wedge} d\mathbf{S}(\wedge)\cdot\mathbf{B} \;=\; \oint_{C_\beta} d\boldsymbol{\ell}(\beta)\cdot\alpha\boldsymbol{\nabla}\beta \;=\; \oint_{C_\beta} d\beta\;\alpha. \tag{3.38}$$

Here, the $\wedge$ subscript is placed on Ψ and a $\wedge$ argument is given for $d\mathbf{S}$ to indicate that this magnetic flux will represent (see below) a magnetic field component orthogonal to both the α and β coordinates. (For example, $d\mathbf{S} \propto \boldsymbol{\nabla}\alpha\times\boldsymbol{\nabla}\beta$.) Because the Clebsch representation is general, we will use this form of the magnetic flux both as a description of the complete magnetic field, and for individual magnetic field components. To obtain the functional dependence of a magnetic flux function it is often simplest to calulate it on a surface where it can be evaluated easily and then extend it to other spatial positions by mapping the magnetic field lines it encompasses to the new positions.

Magnetic flux surfaces can be constructed easily for magnetic configurations or magnetic field components in which there is symmetry (i.e., no dependence on a coordinate) in a direction perpendicular to the magnetic field. Then, we choose β to be that symmetry coordinate, and the magnetic flux and the corresponding vector potential become

$$\Psi_\wedge = \alpha \oint d\beta, \quad \mathbf{A}_\beta = \alpha \boldsymbol{\nabla}\beta = \frac{\Psi_\wedge}{\oint d\beta}\boldsymbol{\nabla}\beta, \quad \text{for symmetry in } \beta. \tag{3.39}$$

When there is symmetry in the β direction, the magnetic field component produced by the component of the vector potential in the $\boldsymbol{\nabla}\beta$ direction can be represented in terms of the corresponding magnetic flux by

$$\mathbf{B}_\wedge = \boldsymbol{\nabla}\times\mathbf{A}_\beta = \boldsymbol{\nabla}\left(\frac{\Psi_\wedge}{\oint d\beta}\right)\times\boldsymbol{\nabla}\beta, \quad \text{for symmetry in } \beta. \tag{3.40}$$

This component of the magnetic field is labeled with a vector cross product subscript ($\wedge$) because it is orthogonal to both the symmetry coordinate and the flux coordinate directions: $\mathbf{B}_\wedge \cdot \boldsymbol{\nabla}\beta = 0$, and $\mathbf{B}_\wedge \cdot \boldsymbol{\nabla}\Psi_\wedge = 0$. Note that $\Psi_\wedge$ is clearly a magnetic flux function since it satisfies (3.37). As a simple example of how to directly use these formulas for a single component magnetic field, Section 3.4 develops the magnetic flux (and Clebsch) coordinates for an axisymmetric magnetic mirror.

These formulas can be used to develop magnetic flux coordinates for the sheared slab model as follows. In the absence of magnetic shear (i.e., for $1/L_S \to 0$), the sheared slab model is symmetric in the y direction. For this case, the dominant or "main" magnetic field component in the sheared slab model can be calculated by taking $\beta = y$, $\oint d\beta = y_0$. Then, we use the rectangular surface in the $z = 0$ plane specified by (see Fig. 3.3a) $0 \le x \le x_0$ and $0 \le y \le y_0$ for calculating the magnetic flux in the z direction to yield $\Psi_z|_{z=0} = \int_0^{x_0} dx \int_0^{y_0} dy\, B_z = (x_0 + x_0^2/2L_B) y_0 B_0$ at $z = 0$. This magnetic flux is extended to other (small) z values using the field line label $x_0 = x - z^2/2R_C$ from (3.14) to yield:

$$\Psi_z \simeq \left(x + \frac{x^2}{2L_B} - \frac{z^2}{2R_C}\right) y_0 B_0 \simeq x\, y_0 B_0, \quad \mathbf{A}_y \equiv \frac{\Psi_y}{y_0}\boldsymbol{\nabla} y,$$
$$\mathbf{B}_{\text{main}} = \boldsymbol{\nabla}\times\mathbf{A}_y = \boldsymbol{\nabla}\left(\frac{\Psi_z}{y_0}\right)\times\hat{\mathbf{e}}_{\text{y}} \simeq B_0\left[\left(1 + \frac{x}{L_B}\right)\hat{\mathbf{e}}_{\text{z}} + \frac{z}{R_C}\,\hat{\mathbf{e}}_{\text{x}}\right]. \tag{3.41}$$

To determine a similar magnetic flux form for the "auxiliary" magnetic shear component in the sheared slab model, we consider the case where the perpendicular gradient in B and curvature are absent (i.e., $1/L_B = 0$ and $1/R_C = 0$), and the field line label simplifies to $x_0 = x$. Then, there is symmetry in the z direction, and we take $\beta = z$, $\oint d\beta = z_0$. Using the rectangular surface in the $y = 0$ plane specified by (see Fig. 3.3b) $0 \le x \le x_0$ and $0 \le z \le z_0$, we obtain $\Psi_y|_{y=0} = -\int_0^{x_0} dx \int_0^{z_0} dz\, B_y = -(x_0^2/2L_S) z_0 B_0$. (The Ψ_y magnetic flux

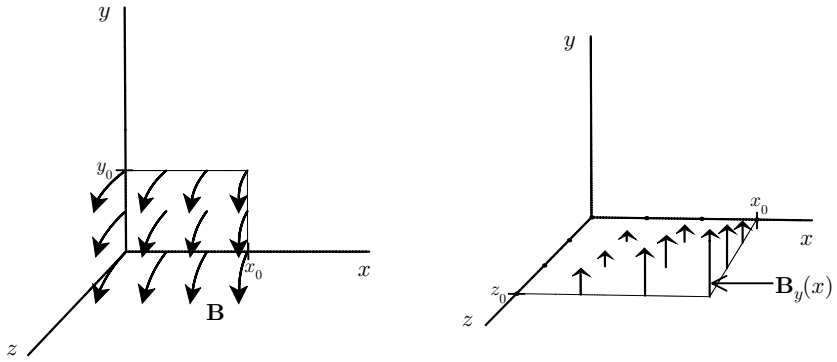

Figure 3.3: Geometry of the surfaces through which the (a) main (Ψ_z) and (b) auxiliary (Ψ_y) magnetic fluxes are calculated for the sheared slab magnetic field model.

is negative because $d\mathbf{S} \equiv d\boldsymbol{\ell}_x \times d\boldsymbol{\ell}_z = \hat{\mathbf{e}}_{\mathrm{x}} dx \times \hat{\mathbf{e}}_{\mathrm{z}} dz = -\hat{\mathbf{e}}_{\mathrm{y}} dx dz$.) Using $x_0 = x$, this yields

$$\Psi_y \;=\; -\,\frac{x^2}{2L_S}\, z_0 B_0, \quad \mathbf{A}_z \;\equiv\; \frac{\Psi_y}{z_0}\boldsymbol{\nabla} z,$$
$$\mathbf{B}_{\mathrm{aux}} \;=\; \boldsymbol{\nabla}\times\mathbf{A}_z \;=\; \boldsymbol{\nabla}\left(\frac{\Psi_y}{z_0}\right)\times \hat{\mathbf{e}}_{\mathrm{z}} \;=\; B_0\,\frac{x}{L_S}\,\hat{\mathbf{e}}_{\mathrm{y}}. \tag{3.42}$$

The total magnetic field in the sheared slab model can be represented in terms of its y and z magnetic flux components by adding these two results:

$$\mathbf{B}_{\mathrm{ss}} \;=\; \mathbf{B}_{\mathrm{main}} + \mathbf{B}_{\mathrm{aux}} \;=\; \boldsymbol{\nabla}(\Psi_z/y_0)\times\boldsymbol{\nabla} y + \boldsymbol{\nabla}(\Psi_y/z_0)\times\boldsymbol{\nabla} z. \tag{3.43}$$

Neglecting terms of order x^2 and z^2, the two components in (3.43) can be combined into a single form $\mathbf{B} \simeq \boldsymbol{\nabla} B_0(x + x^2/2L_B - z^2/2R_C)\times\boldsymbol{\nabla}(y - x\,z/L_S) = \boldsymbol{\nabla}\Psi_z\times\boldsymbol{\nabla} y_0$ using (3.24), which is in the Clebsch form given in (3.34). However, in general the two magnetic flux forms cannot be combined into a single Clebsch form. For the sheared slab model the natural curvilinear coordinates near the origin that can be deduced from this magnetic flux model of the magnetic field are Ψ_z, $y_0 \equiv y - x\,z/L_S$ and $\ell \simeq z$. Note that despite the presence of magnetic shear, curvature and a perpendicular gradient of B, magnetic field lines are, as desired, straight to first order in this magnetic flux coordinate system: $d\Psi_z/d\ell = 0$, $dy_0/d\ell = 0$, and $d\ell \simeq dz$ along field lines.

Many physically relevant situations are more complicated, either because they are fully three-dimensional and have no symmetry direction (e.g., the outer parts of the earth's magnetosphere in Fig. 3.1b and the stellarator in Fig. 3.1e), or because there is a magnetic field component in the symmetry direction(s)

(e.g., the screw pinch in Fig. 3.1e and the tokamak in Fig. 3.1d). When there is more than one magnetic field component and one of the components is in a symmetry direction, the magnetic induction field $\mathbf{B}$ can be written in terms of the magnetic flux components associated with a main (parallel to a symmetry or periodicity direction) and an auxiliary (perpendicular to the dominant symmetry direction, or due to shear, torsion) component of the magnetic field. Each magnetic field component can be written in terms of the relevant magnetic flux in a Clebsch form using (3.40).

In general, representations of $\mathbf{B}$ fields can always be constructed with two magnetic flux functions. They are quite useful in plasma physics. A single or total Clebsch form can be developed from them whenever the two flux functions are single valued functions of each other, which happens when they represent configurations with closed, nested toroidal magnetic flux surfaces. Examples of such systems include axisymmetric toroidal configurations (see Section 3.6) and some regions of stellarators.

For toroidal magnetic configurations with helical magnetic field lines there are two natural cyclic coordinates: the toroidal (long way around the torus) and poloidal (short way) angles ζ and θ. For the moment these will be arbitrarily-defined angles; they are only required to span their respective spaces. Then, in analogy with (3.41) and (3.42), it can be shown in general that the magnetic field can be written in the form of toroidal (tor) and poloidal (pol) magnetic field and flux components:

$$\mathbf{B} \;=\; \mathbf{B}_{\rm tor} + \mathbf{B}_{\rm pol} \;=\; \boldsymbol{\nabla}(\Psi_{\rm tor}/2\pi)\times\boldsymbol{\nabla}\theta + \boldsymbol{\nabla}\zeta\times\boldsymbol{\nabla}(\Psi_{\rm pol}/2\pi). \tag{3.44}$$

The natural sign of the poloidal magnetic flux $\Psi_{\rm pol}$ would be negative for this geometry because of the choice of Ψ, θ, ζ as a right-handed set of coordinates; however, by convention its sign is changed in this definition. The magnetic axis (origin) for the poloidal angle coordinate θ is defined to be the line on which $\mathbf{B}_{\rm pol} \equiv \boldsymbol{\nabla}\zeta\times\boldsymbol{\nabla}(\Psi_{\rm pol}/2\pi)$ vanishes.

In regions where a set of nested toroidal magnetic flux surfaces exist, the poloidal flux function is a single-valued (monotonic) function of the toroidal flux function and hence can be written in terms of it: $\Psi_{\rm pol} = \Psi_{\rm pol}(\Psi_{\rm tor})$. Then, the poloidal and toroidal angles can be modified ($\theta \to \theta_{\rm f}$ and $\zeta \to \zeta_{\rm f}$), so that magnetic field lines are "straight" in them (hence, the f subscript indicating proper *flux* surface coordinates). (See Section 3.6 for the development of such straight-field-line coordinates for axisymmetric toroidal configurations.) Thus, for toroidal configurations with nested flux surfaces, the magnetic field in (3.44) can be written compactly in the Clebsch form

$$\boxed{\mathbf{B} \;=\; \boldsymbol{\nabla}\left(\frac{\Psi_{\rm tor}}{2\pi}\right)\times\boldsymbol{\nabla}\left[\,\theta_{\rm f} - \left(\frac{\iota}{2\pi}\right)\zeta_{\rm f}\,\right], \quad \text{toroidal flux surfaces } \mathbf{B} \text{ field,}} \tag{3.45}$$

where we have defined

$$\boxed{\iota(\Psi_{\rm tor}) \equiv 2\pi \left(\frac{d\Psi_{\rm pol}}{d\Psi_{\rm tor}}\right), \quad \text{rotational transform angle (degrees),}} \tag{3.46}$$

which is the slope $(d\theta_{\rm f}/d\zeta_{\rm f})$ of the magnetic field lines in the $\theta_{\rm f}$–$\zeta_{\rm f}$ plane. Here, ι is the small Greek letter iota; it is divided by 2π in many formulas to represent the angle of field line rotation (per toroidal transit) in radians. For this model magnetic field we identify the Clebsch coordinates as $\alpha = \Psi_{\rm tor}/2\pi$ and $\beta = \theta_{\rm f} - (\iota/2\pi)\,\zeta_{\rm f}$. Along magnetic field lines we have $d\alpha = d\Psi_{\rm tor}/2\pi = 0$ and $d\beta = 0$ or $d\theta_{\rm f} = (\iota/2\pi)\,d\zeta_{\rm f} \Longrightarrow \theta_{\rm f} = (\iota/2\pi)\,\zeta_{\rm f} +$ constant. Thus, magnetic field lines are straight in the $\Psi_{\rm tor}$ =constant, $\theta_{\rm f}$– $\zeta_{\rm f}$ plane. For such toroidal configurations the natural magnetic field curvilinear coordinates are those based on the magnetic flux coordinates $\Psi_{\rm tor}$, $\theta_{\rm f}$, and $\zeta_{\rm f}$, which unfortunately are not usually orthogonal. Nonetheless, since $\iota/2\pi$ is typically not a rational number (ratio of integers, see Section 3.6), the magnetic flux coordinates usually provide a more useful description than the Clebsch coordinates — because of the multivaluedness of the β coordinate in $\theta_{\rm f}$ and $\zeta_{\rm f}$ and because ℓ (or some other coordinate along field lines) is not one of the natural coordinates of the magnetic field description.

3.3 Magnetic Islands

This section will explain how an error magnetic field can create a magnetic island in a sheared magnetic field model — it is yet to be written and inserted. The main point of this section will be to show that when a resonant magnetic field perturbation of the type $\tilde{B}_x = -\hat{B}_x \sin ky$ is added to the sheared slab model it produces a magnetic island of width $w = 4\,(L_S \hat{B}_x/kB_0)^{1/2}$ and to elucidate various properties of field lines in and around the magnetic island structure.

3.4 Open Magnetic Configurations*

There are many types of open magnetic configurations: a cylindrical column of magnetized plasma, magnetic mirrors (Fig. 3.1a), the earth's magnetosphere (Fig. 3.1b), the interplanetary magnetic field, solar flares, cusps (produced by pairs of mirror coils in which the coil currents flow in opposite directions), and so-called divertor regions on open field lines that are outside the closed flux surfaces in toroidal configurations. The simplest and conceptually most important open configurations are of the axisymmetric magnetic mirror type, as shown in Fig. 3.4.

We consider first an axisymmetric magnetic mirror composed of two identical current-carrying solenoidal coils separated by a distance L, as shown in Fig. 3.4a. This "simple mirror" is an important paradigm for discussing many effects of geometry on magnetized plasmas. Since there is symmetry in the azimuthal (θ)

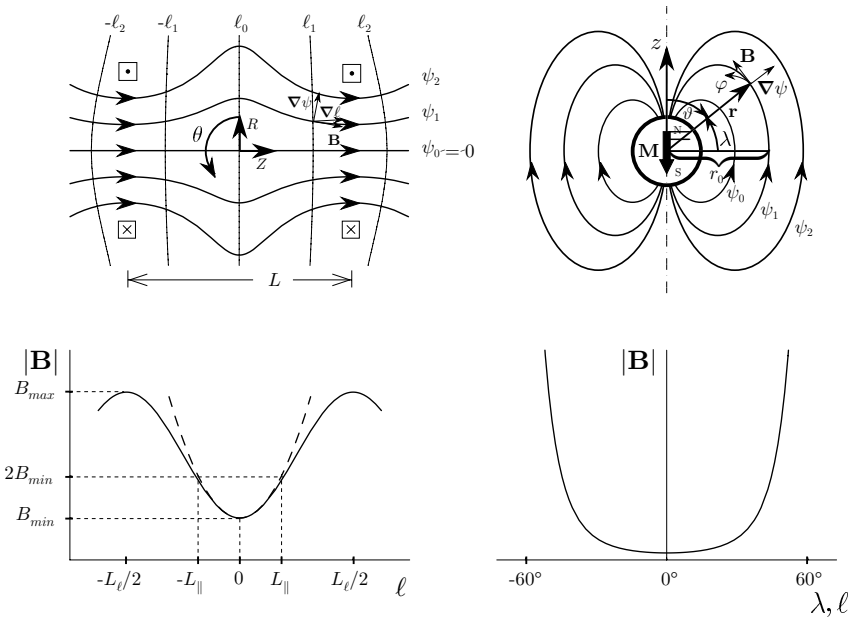

Figure 3.4: Two fundamental types of axisymmetric open magnetic field configurations: a) (on left) axisymmetric or simple magnetic mirror; and b) (on right) a dipole magnetic field such as that due to the earth's magnetic dipole.

direction and no component of $\mathbf{B}$ in this direction, we can construct a Clebsch-type magnetic flux coordinate system using (3.39) and (3.40):

$$\boxed{\mathbf{B} = \boldsymbol{\nabla}\left(\frac{\Psi_m}{2\pi}\right)\times\boldsymbol{\nabla}\theta, \quad \text{axisymmetric mirror (m) magnetic field.}} \tag{3.47}$$

Here, we have taken $\beta = \theta$ and used (3.39) to identify the magnetic flux for an axisymmetric magnetic mirror as $\Psi_m = \alpha \oint d\theta = 2\pi\alpha$. A vector potential that produces this magnetic field is $\mathbf{A} = (\Psi_m/2\pi)\boldsymbol{\nabla}\theta = (\Psi_m/2\pi R)\,\hat{\mathbf{e}}_\theta$. This representation can also be used to describe the "bumpy cylinder" magnetic field produced by a set of solenoidal coils confining a cylindrical column of magnetized plasma (see Problems 3.1 and 3.12).

The magnetic field structure in an axisymmetric magnetic mirror is one of the simplest nontrivial magnetic configurations. In particular, as can be seen from Fig. 3.4a, because of the axisymmetry, it has no gradient of B or curvature in the azimuthal (θ) direction, Also, it has no shear or torsion. However, there are axial (and parallel) and radial gradients of B in an axisymmetric mirror. Further, the magnetic field lines have normal (see Section D.6) curvature ($\kappa_{\mathsf{N}} \propto \boldsymbol{\nabla}\Psi_m \cdot \boldsymbol{\kappa} \neq 0$). When the sheared slab model in (3.8) is used to describe the

local magnetic field in a simple mirror, we make the following associations: $(x, y, z) \to (\Psi_m, \theta, \ell)$, $1/R_C = \kappa_x \to \boldsymbol{\nabla}\Psi_m \cdot \boldsymbol{\kappa}/|\boldsymbol{\nabla}\Psi_m|$, $1/L_B = (1/B)(dB/dx)$ $\to |\boldsymbol{\nabla}\Psi_m|(1/B)(\partial B/\partial \Psi_m)$, $1/L_S \to 0$.

In a simple mirror the magnetic field strength varies significantly along magnetic field lines. It is smallest at the midplane ($Z = 0$) between the mirrors and maximum in the mirror "throats" ($Z = \pm L/2$) of the two coils. Since the variation of $|\mathbf{B}|$ along magnetic field lines is approximately sinusoidal between the mirror coils, it is commonly represented by the sinusoidal model in (3.6). Near the midplane at $\ell = Z = 0$, to lowest order the variation of the magnetic field strength is quadratic in ℓ and can be represented by the quadratic well model (3.4). The mirror ratio $R_m \equiv B_{\max}/B_{\min}$ increases with minor radius R from its minimum on the axis of symmetry ($R = 0$). When the mirror coils are separated by approximately their diameters, its on-axis value is about 2–3.

The magnetic flux coordinate system Ψ_m, θ, ℓ for a simple mirror can be related to a cylindrical coordinate system R, θ, Z constructed about the symmetry axis of the magnetic mirror. For simplicity we define $\ell = 0, Z = 0$ at the midplane between the two mirror coils. We calculate the relation between the distance ℓ along a field line and the axial cylindrical coordinate Z as follows. First, we take the dot product of the field line equation (3.28) with $\hat{\mathbf{e}}_Z \equiv \boldsymbol{\nabla} Z$ to obtain

$$\frac{dZ}{d\ell} \;=\; \frac{B_Z}{B}. \tag{3.48}$$

Since there is no azimuthal magnetic field component ($B_\theta \equiv \hat{\mathbf{e}}_\theta \cdot \mathbf{B} = 0$) and near the axis of symmetry ($R = 0$) we can see from Fig. 3.4a that $B_R << B_Z$, we have

$$B \;=\; \sqrt{B_Z^2 + B_R^2} \;\simeq\; B_Z[1 + (1/2)(B_R^2/B_Z^2) + \cdots]. \tag{3.49}$$

Now, the cylindrical coordinate form of $\boldsymbol{\nabla}\cdot\mathbf{B} = 0$ is

$$\frac{1}{R}\frac{\partial}{\partial R}(RB_R) + \frac{\partial B_Z}{\partial Z} \;=\; 0.$$

Integrating this equation over a small distance R at constant Z away from $R = 0$ where $B_R = 0$ (by axisymmetry) assuming that, as will be demonstrated below, B_Z depends only weakly on R, yields

$$B_R \;\simeq\; -\frac{R}{2}\frac{\partial B_Z}{\partial Z} \;\simeq\; -\frac{R}{2}\frac{\partial B}{\partial \ell} \;\simeq\; -\frac{R\ell}{L_\parallel^2}B_{\min}. \tag{3.50}$$

Here, we have anticipated from (3.49) that $B \simeq B_Z$ and $\ell \simeq Z$ near $R = 0, Z = 0$, and in the last form we have used the quadratic well approximation of (3.4). The radial magnetic field component B_R is nonzero and negative to provide the needed (for $\boldsymbol{\nabla}\cdot\mathbf{B} = 0$) convergence ($dR/d\ell \propto B_R < 0$) of the field lines as the magnetic field strength increases away from the mirror midplane

$(\partial B/\partial \ell > 0)$ — see discussion after (3.3). Using (3.50) in (3.48), the length ℓ along a magnetic field line is given for small R ($<< L_\parallel$) and ℓ ($<< L_\parallel$) by

$$\frac{d\ell}{dZ} = 1 + \frac{1}{2}\frac{B_R^2}{B_Z^2} + \cdots \qquad \Longrightarrow \qquad \ell = Z[1 + R^2Z^2/6L_\parallel^4 + \cdots],$$
$$\boldsymbol{\nabla}\ell = \hat{\mathbf{e}}_Z(1 + R^2Z^2/2L_\parallel^4 + \cdots) + \hat{\mathbf{e}}_R(RZ^3/3L_\parallel^4 + \cdots). \tag{3.51}$$

Note that for $R \neq 0$ the distance ℓ along field lines is longer than the axial distance Z, and that this lengthening effect increases with the cylindrical radius R. Note also that for this simple mirror $\boldsymbol{\nabla}\ell$ does not point in the same direction as $\mathbf{B}$ since the coefficient of $\hat{\mathbf{e}}_R$ in $\boldsymbol{\nabla}\ell$ is positive while $B_R < 0$.

The total magnetic flux Ψ_m within a cylindrical radius R can be determined approximately at the $Z = 0$ plane by neglecting the slight variation of B with R, and then extended along field lines using $R \to R(\ell)$ and $B(Z = 0) \to B(\ell)$:

$$\Psi_m \equiv \iint_{Z=0} d\mathbf{S}\cdot\mathbf{B} = \int_0^{2\pi} d\theta \int_0^R R'dR'B \simeq \pi R^2 B(Z=0) = \pi R^2(\ell)B(\ell). \tag{3.52}$$

The gradient of Ψ_m, which defines one of the directions in the magnetic flux coordinate system, is

$$\boldsymbol{\nabla}(\Psi_m/2\pi) \simeq BR\,\boldsymbol{\nabla}R + (R^2/2)(\partial B/\partial Z)\boldsymbol{\nabla}Z \simeq BR\,[\,\hat{\mathbf{e}}_R + (RZ/L_\parallel^2)\,\hat{\mathbf{e}}_Z].$$

Using this result together with $\boldsymbol{\nabla}\theta = \hat{\mathbf{e}}_\theta/R$ in (3.47) yields the desired magnetic field direction and magnitude variation along field lines for an axisymmetric mirror near $R = 0, Z = 0$.

The magnetic flux within a given bundle of magnetic field lines is conserved (since $\mathbf{B}\cdot\boldsymbol{\nabla}\Psi_m = 0$) as we move along the field lines and the magnetic field strength varies. Thus, the radius $R(\ell)$ of a given magnetic flux surface (or field line) can be determined from (3.52),

$$\boxed{R(\ell) \simeq \sqrt{\frac{\Psi_m}{\pi B(\ell)}} = R(0)\sqrt{\frac{B_{\min}}{B(\ell)}}, \quad \text{radius of flux surface.}} \tag{3.53}$$

Hence, the radius of a flux surface varies inversely with the square root of the field strength — flux surfaces get smaller in radius R as we move toward the mirror throats.

The normal ($\boldsymbol{\nabla}\Psi_m$ or radial direction) curvature of the magnetic field lines can be obtained from the second derivative of $R(\ell)$ along a field line: $\kappa_R \equiv d^2R(\ell)/d\ell^2$. Near the axis of symmetry and midplane of a simple mirror it is given by

$$\kappa_R \simeq -R/L_\parallel^2, \quad \text{for } R, |Z| << L_\parallel. \tag{3.54}$$

[This result can also be obtained from the definition $\kappa_R \equiv d(B_R/B)/d\ell$ from (3.15) — see Problem 3.11]. Thus, as is obvious physically from the axisymmetric magnetic mirror geometry, the radius of curvature $R_C \equiv 1/|\kappa_R|$ is infinite on the symmetry axis ($R = 0$), but is finite for $R \neq 0$ and decreases as R increases.

The variation of $|\mathbf{B}|$ in the radial (R) direction can be estimated from the magnetic field curvature as follows. First, we recall that for small R, Z the magnetic field can be expanded as indicated in (3.49). Next, we assume that the plasma electrical current in the θ direction is small and can be neglected. Then, the θ component of the equilibrium ($\partial/\partial t \to 0$) Ampere's law becomes

$$0 = \hat{\mathbf{e}}_\theta \cdot \boldsymbol{\nabla} \times \mathbf{B} = \frac{\partial B_R}{\partial Z} - \frac{\partial B_Z}{\partial R} \simeq B_Z(\kappa_R - \frac{\partial \ln B_Z}{\partial R}).$$

Thus, as we could also have deduced from (3.18), we have

$$\frac{\partial \ln B_Z}{\partial R} \simeq \kappa_R \simeq -\frac{R}{L_\parallel^2} \qquad \Longrightarrow \qquad B_Z \simeq B_{\min}\left(1 + \frac{Z^2}{L_\parallel^2} - \frac{R^2}{2L_\parallel^2}\right). \tag{3.55}$$

Using this result in the expression for $|\mathbf{B}|$ in (3.49), we find

$$\boxed{|\mathbf{B}| \simeq B_{\min}\left[\left(1 + \frac{\ell^2}{L_\parallel^2}\right)\left(1 - \frac{R^2}{2L_\parallel^2}\right) + \cdots\right].} \tag{3.56}$$

Hence, as can be discerned by looking at the density of the field lines sketched in Fig. 3.4a, there is a saddle point in the magnetic field strength at the center ($R = 0$, $Z = \ell = 0$) of the simple mirror — $|B|$ increases along field lines ($\partial^2 B/\partial \ell^2 > 0$ near $|Z| = 0$), but decreases radially ($\partial B/\partial R < 0$, for $R \neq 0$). Within the axisymmetric model of the magnetic mirror field, $|\mathbf{B}|$ always decreases with radius R; hence the region near $R = 0$, $Z = 0$ is a "magnetic hill" radially, but a "magnetic well" axially. It will turn out (see Chapter 21) that for macroscopic plasma stability we need to place the plasma in a global magnetic well ($\partial B/\partial R > 0$, $\partial^2 B/\partial Z^2 > 0$). A "minimum-B" or "magnetic well" mirror configuration can be created by adding nonaxisymmetric, multipolar magnetic fields that are produced by currents in alternating directions in a set of axial wires ("Ioffe bars") outside the mirror coils (see Section 21.1).

Next, we consider the axisymmetric magnetic field generated by the earth's magnetic dipole, as indicated in Fig. 3.4b. Since the electrical currents in the plasma near the earth are too weak to significantly affect the magnetic field, we need only calculate the vacuum field induced by the earth's dipole magnetic moment $\boldsymbol{\mu}_E \equiv -M_d\,\hat{\mathbf{e}}_z$. The magnetic potential Φ_d induced by a point magnetic dipole is given by ($\{\mu_0/4\pi\} \to 1$ for mks $\to$ cgs units)

$$\Phi_d = \left\{\frac{\mu_0}{4\pi}\right\} \frac{\boldsymbol{\mu}_E \cdot \mathbf{x}}{|\mathbf{x}|^3}, \quad \text{magnetic potential for dipole field.} \tag{3.57}$$

Using the spherical coordinate system shown in Fig. 3.4b, outside the earth ($r > R_E$) the magnetic potential becomes

$$\Phi_d = -\left\{\frac{\mu_0}{4\pi}\right\} \frac{M_d\,\hat{\mathbf{e}}_z \cdot \mathbf{x}}{|\mathbf{x}|^3} = -\left\{\frac{\mu_0}{4\pi}\right\} \frac{M_d \sin\lambda}{r^2} \tag{3.58}$$

in which $|\mathbf{x}| = r$ is the distance from the center of the earth. Here, we have used $\hat{\mathbf{e}}_z \cdot \mathbf{x} = z = r\cos\vartheta = r\sin\lambda$ in which $\lambda = \pi/2 - \vartheta$ is the angle characterizing the latitude from the equatorial plane ($\vartheta = \pi/2$, $\lambda = 0$).

Evaluating the components of $\mathbf{B} = -\boldsymbol{\nabla}\Phi_d$ in r, λ, φ spherical coordinates, we obtain

$$B_r \,=\, -\left\{\frac{\mu_0}{4\pi}\right\}\frac{2\,M_d\sin\lambda}{r^3}, \quad B_\lambda \,=\, \left\{\frac{\mu_0}{4\pi}\right\}\frac{M_d\cos\lambda}{r^3}, \quad B_\varphi \,=\, 0, \quad \text{diplole field.} \tag{3.59}$$

The B_φ component vanishes because of the axisymmetry about the earth's magnetic axis. The total magnetic field strength is thus given by

$$B \,=\, \sqrt{B_r^2 + B_\lambda^2} \,=\, \left\{\frac{\mu_0}{4\pi}\right\}\frac{M_d\,(1+3\sin^2\lambda)^{1/2}}{r^3}, \tag{3.60}$$

which shows that the magnetic field strength increases with latitude λ and decreases with radial distance (as $1/r^3$).

The magnetic flux Ψ_d for a dipole (subscript d) magnetic field can be calculated from the magnetic field penetrating downward through a disk in the $z =$ constant plane that extends radially outward from r to infinity using $d\mathbf{S}(z) \propto -\,\hat{\mathbf{e}}_z$, and $\mathbf{B}\cdot(-\,\hat{\mathbf{e}}_z) = -B_\lambda\cos\lambda$:

$$\Psi_d \,=\, \iint d\mathbf{S}(z)\cdot\mathbf{B} \,=\, -\int_r^\infty r'dr'\int_0^{2\pi} d\varphi\,\cos\lambda\,B_\lambda \,=\, -\left\{\frac{\mu_0}{4\pi}\right\}\frac{2\pi M_d\cos^2\lambda}{r}. \tag{3.61}$$

The direction of $d\mathbf{S}(z)$ and sign of Ψ_d were chosen so that $\boldsymbol{\nabla}\Psi_d$ is in the $\hat{\mathbf{e}}_r$ (radially outward) direction at $\lambda = 0$. The variation of the radius of a field line as λ changes can be obtained from the constancy of the magnetic flux Ψ_d along field lines: $r(\lambda) = r_0\cos^2\lambda$ in which r_0 is the radius of the field line in the equatorial plane. Using this field line result in (3.60), we find that along a magnetic field line $|\mathbf{B}| \propto (1+3\sin^2\lambda)^{1/2}/\cos^6\lambda$, which increases rapidly away from the equator ($\lambda = 0$) — see Fig. 3.4b. Near the equatorial plane the magnetic field strength can be modeled by the quadratic well model of (3.4) with $\ell \simeq r_0\lambda$ and $L_\parallel = (\sqrt{2}/3)r_0$ (see Problem 3.14). Since $\partial B/\partial\ell > 0$ for $\ell > 0$, magnetic field unit vectors converge ($B_r < 0$, $\boldsymbol{\nabla}\cdot\hat{\mathbf{b}} < 0$) as we move along field lines vertically, above and away from the equatorial plane, toward the earth's polar regions where the magnetic field strength is largest.

For a Clebsch-type magnetic flux representation of the dipole magnetic field we take $\beta \to \varphi$ and $\alpha \to \Psi/2\pi$, and thus have

$$\boxed{\mathbf{B} = \boldsymbol{\nabla}\left(\frac{\Psi_d}{2\pi}\right)\times\boldsymbol{\nabla}\varphi, \quad \text{dipole magnetic field.}} \tag{3.62}$$

That this form reproduces the field components in (3.59) can be shown using $\boldsymbol{\nabla}\varphi = \hat{\mathbf{e}}_\varphi/(r\cos\lambda)$, $\hat{\mathbf{e}}_r\times\hat{\mathbf{e}}_\varphi = \hat{\mathbf{e}}_\lambda$, $\hat{\mathbf{e}}_\lambda\times\hat{\mathbf{e}}_\varphi = -\,\hat{\mathbf{e}}_r$ (because $\lambda = \pi/2 - \vartheta$). Note

also that the dipole magnetic field can be represented by the vector potential $\mathbf{A} = (\Psi_d/2\pi)\boldsymbol{\nabla}\varphi = (\Psi_d/2\pi r)\,\hat{\mathbf{e}}_\varphi$.

Like the simple mirror, the earth's dipole magnetic field has no shear or torsion. However, there is normal (radial) curvature and, since this is a nearly vacuum field, a concomitant radial gradient of $|\mathbf{B}|$. Using (3.60) and $\mathbf{J} \simeq \mathbf{0}$ in (3.20), we find for all λ

$$\kappa_r = \frac{\partial}{\partial r}\ln B = -\frac{3}{r}, \quad L_B = R_C = \frac{r}{3}, \quad \text{curvature of vacuum dipole field.} \tag{3.63}$$

Note that for the dipole field the radius of curvature is independent of latitude λ and equal to its obvious value of $-3/r$ in the equatorial plane ($\lambda = 0$). When the sheared slab model in (3.8) is used to describe the local magnetic field in the earth's dipole field, we make the following associations: $(x, y, z) \to (\Psi, \varphi, \ell)$, $1/L_B \to \kappa_r$, $\kappa_x \to \kappa_r$, and $1/L_S = 0$.

Since mathematical descriptions of nonaxisymmetric open magnetic configurations usually depend on the specifics of the particular case, we will not develop any in detail. While the characteristics of particular open magnetic configurations can be quite important for specific effects, the lowest order or most fundamental properties of open configurations are usually dominated by the open rather than closed nature of the field lines, the magnetic mirrors along $\mathbf{B}$, and the $\boldsymbol{\nabla}B$ and curvature of the field lines. These latter properties are all included in the axisymmetric models developed above. Thus, the axisymmetric simple mirror or dipole field models provide appropriate lowest order magnetic field models for all open configurations.

3.5 Screw Pinch Model*

There are a number of types of axisymmetric toroidal magnetic field configurations used for plasma confinement: tokamaks (Fig. 3.1d), spherical tokamaks, spheromaks and reversed field pinches — devices whose interrelationships are discussed at the end of this and the next section. The paradigm for the axisymmetric toroidal class of configurations is the tokamak, both because it is the simplest axisymmetric toroidal magnetic configuration with two magnetic field components, and because so many experimental tokamaks have been built and operated worldwide in the pursuit of the magnetic confinement approach to controlled fusion. In turn, the tokamak magnetic geometry is often approximated by a periodic cylinder (see Fig. 3.1c), which is called the screw pinch model and the focus of this section. In this section and the following one we develop the screw pinch and axisymmetric toroidal models in general, and then indicate the lowest order tokamak forms in the usual large aspect ratio (thin donut) expansion after approximate equalities ($\simeq$). The use and forms of these general magnetic field structures for other axisymmetric toroidal configurations are discussed at the end of the sections: reversed field pinches at the end of this section, and spherical tokamaks and spheromaks at the end of the next section.

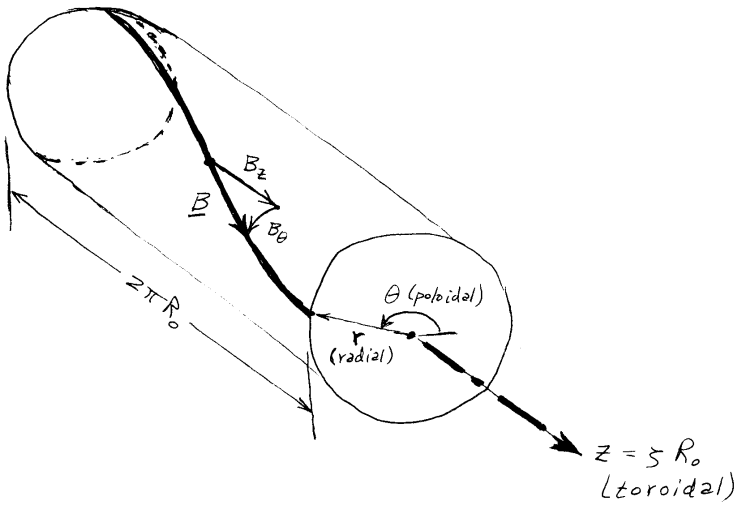

Figure 3.5: Screw pinch model of tokamak magnetic field geometry. The axial periodicity length $2\pi R_0$ represents the periodicity of the tokamak in the toroidal direction.

The key parameter that describes the degree of toroidicity in all toroidal magnetic configurations is the reciprocal of the aspect ratio. The aspect ratio A is defined as the ratio of the major (R_0) to minor (r) radius of a given magnetic flux surface in the torus. The degree of toroidicity in toroidal configurations is indicated by the parameter

$$\boxed{\epsilon \equiv \frac{r}{R_0} = \frac{1}{A}, \quad \text{inverse aspect ratio.}} \tag{3.64}$$

This is a "small" number for magnetic flux surfaces inside most standard tokamaks whose aspect ratios at the plasma edge typically range from 2.5 to 5. Thus, it will be used as an expansion parameter in the analysis of tokamak magnetic field systems.

There are two classes of intrinsically toroidal effects in tokamaks that need to be taken into account for small but finite ϵ. First, there are the effects due to the toroidal curvature: the toroidal curvature of the magnetic field lines and the differences in the magnetic field strength on the inner (small R) and outer (large R) sides of the torus [see Eq. (3.110) in the next section]. Second, and most importantly, there is the double periodicity of the system — in the toroidal (long way around the torus) and poloidal (short way) angle variables ζ and θ.

In the screw pinch (periodic cylinder) model of the tokamak the double periodicity is taken into account, but the toroidal curvature effects are neglected. This model uses an r, θ, z cylindical geometry, as indicated in Fig. 3.5. In the screw pinch model, r reresents the minor radius (or flux surface label) and θ

represents the poloidal angle in the tokamak. The tokamak's periodicity in the toroidal angle ζ is modeled by requiring periodicity in the axial coordinate z over the toroidal length of the torus, $2\pi R_0$. Thus, the axial distance z in the screw pinch is associated with the tokamak toroidal angle ζ through

$$z \,=\, \zeta\, R_0. \tag{3.65}$$

The magnetic field in a tokamak has two components. The main, toroidal (ζ, z) magnetic field $\mathbf{B}_{\rm tor}$ is produced by electrical currents flowing poloidally — mainly in coils wrapped poloidally around the torus, but also within the plasma. The smaller (for $\epsilon << 1$) poloidal (θ) magnetic field $\mathbf{B}_{\rm pol}$ is produced by the toroidal component of current flowing in the plasma. In the screw pinch model both components can depend on the minor radius r, although the variation of $|\mathbf{B}_{\rm tor}|$ with r is weak for typical tokamaks. Thus, the magnetic field in a tokamak is modeled by

$$\boxed{\mathbf{B} \,=\, \mathbf{B}_{\rm tor} + \mathbf{B}_{\rm pol} \,\equiv\, B_z(r)\,\hat{\mathbf{e}}_{\rm z} + B_\theta(r)\,\hat{\mathbf{e}}_\theta, \quad \text{screw pinch model field.}} \tag{3.66}$$

Note that in the screw pinch model there is symmetry in the z, θ directions and magnetic field lines lie on constant radius (r) surfaces ($\hat{\mathbf{e}}_r \cdot d\mathbf{x}/d\ell = B_r/B = 0$).

The poloidal magnetic field is related to the axial component of the current density $\mathbf{J}$ through the axial component of the equilibrium Ampere's law:

$$\hat{\mathbf{e}}_{\rm z} \cdot \boldsymbol{\nabla}\times\mathbf{B} = \mu_0\, \hat{\mathbf{e}}_{\rm z} \cdot \mathbf{J} \qquad \Longrightarrow \qquad \frac{1}{r}\frac{d}{dr}\left[\, rB_\theta(r)\,\right] = \mu_0 J_z(r). \tag{3.67}$$

Integrating this equation using the boundary condition (by symmetry) that $B_\theta = 0$ at $r = 0$ yields

$$B_\theta(r) \,=\, \frac{\mu_0}{r}\int_0^r r'dr' J_z(r') \,=\, \frac{\mu_0 I_z(r)}{2\pi r}, \quad \text{poloidal magnetic field,} \tag{3.68}$$

in which $I_z(r) \,\equiv\, \iint d\mathbf{S}(z)\cdot\mathbf{J}$ is the axial current flowing within a radius r. Similarly, the radial variation of the toroidal magnetic field B_z is related to the poloidal current density through $\hat{\mathbf{e}}_\theta \cdot \boldsymbol{\nabla}\times\mathbf{B} = \mu_0 J_\theta \Longrightarrow -\,dB_z/dr = \mu_0 J_\theta$, which upon integration using the boundary condition that the currents in the external poloidal coils and the plasma produce a toroidal magnetic field strength of $B_z(0) \equiv B_0$ on the axis $(r = 0)$ yields

$$B_z(r) \,=\, B_0\left[1 - \frac{\mu_0}{B_0}\int_0^r dr' J_\theta(r')\right] \,\simeq\, B_0, \quad \text{toroidal magnetic field.} \tag{3.69}$$

In order to determine the radial dependence of B_z, we need a specific plasma model for the poloidal current density J_θ. However, as indicated by the approximate equality, the magnetic field induced by the poloidal current in a tokamak is usually small — because the helical pitch [see (3.73) below] of the field lines is small, and because the plasma-pressure-induced currents are small for low pressure plasmas.

The magnetic fluxes associated with the toroidal and poloidal magnetic fields in the screw pinch model can be determined by calculating the magnetic fluxes in the z and θ symmetry directions (see Fig. 3.5):

$$\Psi_{\rm tor} \equiv \iint d\mathbf{S}(z)\cdot\mathbf{B}_{\rm tor} = 2\pi\int_0^r r'dr'B_z(r'), \quad \text{toroidal magnetic flux,} \tag{3.70}$$

$$\Psi_{\rm pol} \equiv \iint d\mathbf{S}(\theta)\cdot\mathbf{B}_{\rm pol} = 2\pi R_0\int_0^r dr'B_\theta(r'), \quad \text{poloidal magnetic flux.} \tag{3.71}$$

The screw pinch magnetic field (3.66) can be written in terms of these magnetic fluxes using (3.40) or $\mathbf{A} = (\Psi_{\rm tor}/2\pi)\boldsymbol{\nabla}\theta - (\Psi_{\rm pol}/2\pi)\boldsymbol{\nabla}(z/R_0)$:

$$\begin{aligned}\mathbf{B} &= \boldsymbol{\nabla}(\Psi_{\rm tor}/2\pi)\times\boldsymbol{\nabla}\theta + \boldsymbol{\nabla}(z/R_0)\times\boldsymbol{\nabla}(\Psi_{\rm pol}/2\pi)\\ &= \boldsymbol{\nabla}(\Psi_{\rm tor}/2\pi)\times\boldsymbol{\nabla}[\theta - (\iota/2\pi)\,(z/R_0)]\end{aligned} \tag{3.72}$$

in which we have used the definition of $\iota = \iota(r)$ in (3.46). The last form is a Clebsch representation with $\alpha = \Psi_{\rm tor}/2\pi$ and $\beta = \theta - (\iota/2\pi)\,(z/R_0)$. For this Clebsch representation, the equation for a magnetic field line is $d\alpha = 0 \Longrightarrow \Psi_{\rm tor}(r) = \text{constant} \Longrightarrow r = \text{constant}$ and $d\beta = 0 \Longrightarrow d\theta = (\iota/2\pi)\,dz/R_0 \Longrightarrow \theta = z\,(\iota/2\pi R_0) + \text{constant}$. Thus, the magnetic field lines in a screw pinch lie on r = constant surfaces and are naturally straight in the θ–z plane with a constant helical pitch (see Fig. 3.1c):

$$\frac{d\theta}{dz} = \frac{\iota(r)}{2\pi R_0}, \quad \text{helical pitch of field lines.} \tag{3.73}$$

Note that the screw pinch model magnetic field is in the toroidal flux form of (3.45) with the straight field line coordinates identified as $\theta_{\rm f} \to \theta$ and $\zeta_{\rm f} \to z/R_0$.

It is customary to characterize the inverse of the pitch of the helix of magnetic field lines in a tokamak by a global measure (see Fig. 3.8 and discussion in next section) which is the number of toroidal (or axial periodicity length) transits of a magnetic field line per poloidal transit (θ increasing from 0 to 2π):

$$\boxed{q(r) \equiv \frac{\#\text{ toroidal transits of a field line}}{\#\text{ poloidal transits of a field line}}, \quad \text{toroidal winding number}}$$

$$= \frac{\int_0^{2\pi R_0/(\iota/2\pi)} dz/2\pi R_0}{\int_0^{2\pi} d\theta/2\pi} = \frac{2\pi}{\iota(r)} = \frac{d\Psi_{\rm tor}}{d\Psi_{\rm pol}} = \frac{r\,B_z(r)}{R_0 B_\theta(r)}. \tag{3.74}$$

The q value is also known as the "safety factor" because, as we will see in Chapter 21, it must be greater than unity for macroscopic plasma stability in a tokamak. Typical radial profiles for the poloidal and toroidal currents and magnetic fields and the consequent q profile are shown in Fig. 3.6. As indicated, q typically ranges from about unity on axis to a value of 3–5 at the plasma edge. In terms of q the helical pitch of the field lines in (3.73) becomes simply $d\theta/dz = 1/R_0 q$.

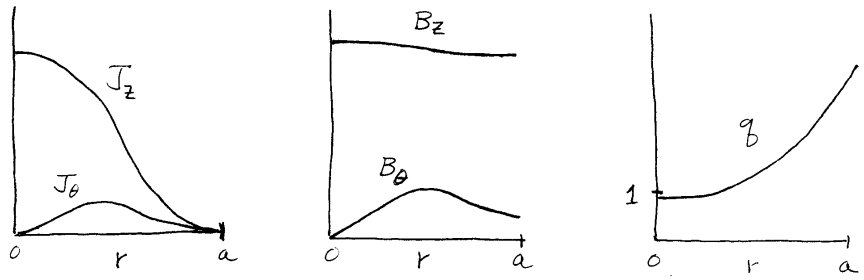

Figure 3.6: Radial profiles for a typical large aspect ratio tokamak: a) currents, b) magnetic fields, and c) toroidal winding number q.

It is also customary in tokamaks to use the poloidal rather than toroidal magnetic flux as the radial variable and to leave out the 2π factor by defining

$$\boxed{\psi \equiv \frac{\Psi_{\rm pol}}{2\pi} = R_0 \int_0^r dr'\, B_\theta(r'), \quad \boldsymbol{\nabla}\psi = R_0 B_\theta(r)\,\hat{\mathbf{e}}_r, \quad \text{poloidal flux function.}} \tag{3.75}$$

Thus, the normal magnetic flux representation of the screw pinch model for a tokamak is

$$\mathbf{B} = \boldsymbol{\nabla}\psi\times\boldsymbol{\nabla}(q\theta - z/R_0) \simeq B_0\,\hat{\mathbf{e}}_z + \hat{\mathbf{e}}_z\times\boldsymbol{\nabla}\psi, \quad \text{screw pinch field,} \tag{3.76}$$

in which the approximate form indicates the lowest order form in the large aspect ratio limit $\epsilon << 1$. Working out the magnetic field components from either (3.66) or (3.76) using (3.74), we obtain

$$\mathbf{B} \equiv B_z\,\hat{\mathbf{e}}_z + B_\theta\,\hat{\mathbf{e}}_\theta = B_z(r)\left[\hat{\mathbf{e}}_z + \frac{r}{R_0 q(r)}\,\hat{\mathbf{e}}_\theta\right] \simeq B_0\left[\hat{\mathbf{e}}_z + \frac{\epsilon}{q}\,\hat{\mathbf{e}}_\theta\right], \tag{3.77}$$

Note that the total magnetic field strength in this model is

$$B = \sqrt{B_z^2 + B_\theta^2} = B_z\sqrt{1 + B_\theta^2/B_z^2} = B_z h \simeq B_0 \tag{3.78}$$

in which we have defined the geometric factor

$$h \equiv B/B_z = \sqrt{1 + r^2/R_0^2 q^2} = \sqrt{1+\epsilon^2/q^2} \simeq 1. \tag{3.79}$$

For typical tokamaks $\epsilon/q \sim 0.1 << 1$, so usually the poloidal (θ) magnetic field is smaller than the toroidal (dominant) magnetic field by about an order of magnitude. Thus, for typical tokamaks the approximate equalities at the end of equations (3.69), and (3.76)–(3.79) and subsequent ones in this section apply. Note also that hence the helical field lines in typical tokamaks have only a slight twist angle (torsion): $r\,d\theta/dz = r/R_0 q = \epsilon/q << 1$.

In the screw pinch model the magnetic field strength is constant along a magnetic field line; hence from (3.3) the screw pinch model magnetic field unit vectors $\hat{\mathbf{b}} \equiv \mathbf{B}/B$ neither converge or diverge. However, the magnetic field in this model does have torsion, curvature, a perpendicular gradient and shear. For the screw pinch model the unit vector along the magnetic field is

$$\hat{\mathbf{b}} \equiv \frac{\mathbf{B}}{B} = \frac{1}{h}\left(\hat{\mathbf{e}}_z + \frac{r}{R_0 q}\,\hat{\mathbf{e}}_\theta\right) \simeq \left(\hat{\mathbf{e}}_z + \frac{\epsilon}{q}\,\hat{\mathbf{e}}_\theta\right). \tag{3.80}$$

Using the definition of the torsion in (**??**) with a unit normal $\hat{\mathbf{N}} = \boldsymbol{\nabla}\psi/|\boldsymbol{\nabla}\psi| = \hat{\mathbf{e}}_r$, we find that for the screw pinch model

$$\boxed{\boldsymbol{\tau} = -(\hat{\mathbf{b}}\cdot\boldsymbol{\nabla})(\hat{\mathbf{b}}\times\hat{\mathbf{e}}_r) = -\frac{r}{hR_0q}\,(\hat{\mathbf{e}}_\theta\cdot\boldsymbol{\nabla})\frac{\hat{\mathbf{e}}_\theta}{h} = \frac{1}{h^2R_0q}\,\hat{\mathbf{e}}_\theta, \quad \text{torsion.}} \tag{3.81}$$

Here, we have used the vector identities (**??**), (**??**) and (**??**) along with $\boldsymbol{\nabla}\theta = \hat{\mathbf{e}}_\theta/r$ to show that

$$(\hat{\mathbf{e}}_\theta\cdot\boldsymbol{\nabla})\hat{\mathbf{e}}_\theta = -\,\hat{\mathbf{e}}_\theta\times(\boldsymbol{\nabla}\times\hat{\mathbf{e}}_\theta) = -\,\hat{\mathbf{e}}_\theta\times(\boldsymbol{\nabla}\times r\boldsymbol{\nabla}\theta) = -\,\hat{\mathbf{e}}_\theta\times(\hat{\mathbf{e}}_r\times\hat{\mathbf{e}}_\theta)/r = -\,\hat{\mathbf{e}}_r/r; \tag{3.82}$$

hence $\hat{\mathbf{e}}_r\cdot(\hat{\mathbf{e}}_\theta\cdot\boldsymbol{\nabla})\hat{\mathbf{e}}_\theta = -1/r$. Thus, the distance along a magnetic field line over which it twists helically through one radian in the screw pinch model is

$$\boxed{L_\tau = 1/\tau_r = h^2R_0q \simeq R_0q, \quad \text{torsion length.}} \tag{3.83}$$

The torsion vector $\boldsymbol{\tau}$ can also be written in terms of the magnetic field components as $\boldsymbol{\tau} = (B_\theta B_z/rB^2)\,\hat{\mathbf{e}}_r$ — see Problem 3.19. Note also that in the tokamak limit of $\epsilon/q << 1$ the helical pitch of the field lines given in (3.73) becomes simply the torsion τ_r.

The curvature in the screw pinch model is worked out similarly using the vector identities (**??**) and (3.82):

$$\boxed{\boldsymbol{\kappa} \equiv (\hat{\mathbf{b}}\cdot\boldsymbol{\nabla})\hat{\mathbf{b}} = \frac{r}{hR_0q}(\hat{\mathbf{e}}_\theta\cdot\boldsymbol{\nabla})\frac{r}{hR_0q}\,\hat{\mathbf{e}}_\theta = -\frac{r}{(hR_0q)^2}\,\hat{\mathbf{e}}_r, \quad \text{curvature.}} \tag{3.84}$$

The curvature of magnetic field lines in the screw pinch model can be written in terms of the magnetic field components as $\boldsymbol{\kappa} = -(B_\theta^2/rB^2)\,\hat{\mathbf{e}}_r$ — see Problem 3.19. The curvature length $R_C \equiv 1/|\kappa_r| = (hR_0q)^2/r \simeq R_0q(q/\epsilon)$ is much longer than the torsion length $L_\tau \simeq R_0q$ in the screw pinch model of a tokamak because the curvature is produced only by the poloidal motion of the small pitch helical field lines. The perpendicular (radial) gradient scale length $[L_B \equiv B/(dB/dr)]$ is of the order of the curvature radius R_C. However, since the difference depends on the current and plasma pressure profiles, it will not be worked out until Chapter 20. Note also that since the curvature is only in the radial direction there is only normal curvature. Because the magnetic field lines do not have curvature within a magnetic flux surface, there is no geodesic curvature — see (**??**) in Section D.6.

Finally, it can be shown (see Problem 3.25) that for the screw pinch model the local magnetic shear defined in (**??**) and (3.25) becomes (see Problem 3.19 for the form of the magnetic shear in terms of the magnetic field components B_θ and B_z):

$$\varsigma \equiv (\hat{\mathbf{b}}\times\hat{\mathbf{e}}_\mathrm{r})\cdot\boldsymbol{\nabla}\times(\hat{\mathbf{b}}\times\hat{\mathbf{e}}_\mathrm{r}) = \frac{1}{L_S} = \frac{r}{h^2R_0}\frac{d}{dr}\left(\frac{1}{q}\right). \tag{3.85}$$

Note that in the screw pinch model the shear is constant on a magnetic flux surface (r = constant). Recalling from (3.74) that $1/q$ is just the radian rotational transform $\iota/2\pi$ of the helical field lines, the local shear can be written as

$$\boxed{\varsigma = \frac{1}{L_S} = \frac{r}{2\pi h^2R_0}\frac{d\iota}{dr} = -\frac{r}{h^2R_0q^2}\frac{dq}{dr} = -\frac{s}{h^2R_0q} \simeq -\frac{s}{R_0q}, \quad \text{magnetic shear,}} \tag{3.86}$$

in which

$$s(r) \equiv \frac{r}{q}\frac{dq}{dr}, \quad \text{magnetic shear parameter,} \tag{3.87}$$

is an order unity magnetic shear parameter commonly used in stability analyses of tokamak plasmas. There is magnetic shear in large aspect ratio tokamaks only if the axial current density J_z varies with radius r since $\iota \propto B_\theta(r)/r \propto (1/r^2)\int_0^r r'dr'J_z(r')$. By convention, in tokamak plasma analyses the sign of the shear is reversed so that $s > 0$ indicates positive or "normal" magnetic shear, and $s < 0$ indicates reversed or abnormal shear.

Having delineated the local differential properties in the screw pinch model, we can now develop a sheared slab model for it. At finite r since the curvature and perpendicular gradient scale lengths are so long (compared to the torsion and shear lengths) their effects are usually neglected in the simplest slab models. As indicated previously, the sheared slab model does not include torsion effects. Thus, the local sheared slab model for the screw pinch model of a tokamak near a field line at a radius r_0 is simply

$$\mathbf{B}_\mathrm{ss} = B_0\,\hat{\mathbf{b}} + \hat{\mathbf{b}}\times\boldsymbol{\nabla}\psi_\mathrm{aux} = B_0\,[\,\hat{\mathbf{b}} + (x/L_S)\,\hat{\mathbf{e}}_\wedge]. \tag{3.88}$$

in which

$$\psi_\mathrm{aux} \equiv B_0\,\frac{x^2}{2L_S}, \quad \text{and} \quad \hat{\mathbf{e}}_\wedge \equiv \hat{\mathbf{b}}\times\hat{\mathbf{e}}_\mathrm{r} = \frac{1}{h}\left(\hat{\mathbf{e}}_\theta - \frac{\epsilon}{q}\hat{\mathbf{e}}_\mathrm{z}\right) \simeq \left(\hat{\mathbf{e}}_\theta - \frac{\epsilon}{q}\hat{\mathbf{e}}_\mathrm{z}\right). \tag{3.89}$$

Here, the sheared slab model coordinates x, y, z correspond to $r - r_0, r_0[\theta - (\epsilon/q)(z/R_0)], z + (\epsilon/q)r_0\theta$ and we identify the directions in terms of the cylindrical coordinate directions through the directions indicated in the unit vector $\hat{\mathbf{b}}$ in (3.80) and a unit vector $\hat{\mathbf{e}}_\wedge$ that is perpendicular to $\hat{\mathbf{b}}$ within the r = constant (magnetic flux) surface.

The preceding discussion focused on the screw pinch model for tokamaks. The screw pinch model can also be used to represent reversed field pinch (RFP)

plasmas. In RFPs the toroidal and poloidal currents are much larger than those in a tokamak (by a factor $\sim 1/\epsilon \sim A >> 1$). In particular, the poloidal current J_θ is so large that it causes the toroidal magnetic field to reverse direction in the edge of the plasma [see (3.69)] — hence the name of the confinement concept. The toroidal current in an RFP produces a poloidal magnetic field B_θ that is so large that $q \sim \epsilon$ and the small ϵ/q expansion that is used for tokamaks is inappropriate. Such a large poloidal magnetic field also produces an order unity helical pitch of the magnetic field lines; magnetic field lines in an RFP rotate poloidally and toroidally on about the same length scales, and even become a reversed direction helix ($q < 0$) in the edge of the plasma. For such a magnetic field structure the curvature is clearly dominated by the poloidal motion of the field lines; the toroidal curvature effects are higher order. Thus, to lowest order the general [before the approximate equalities ($\simeq$)] screw pinch model developed in this section is often used to approximately describe reversed field pinch plasmas. When a more precise description including toroidicity effects is needed the full magnetic flux description developed in the following section must be used.

3.6 Axisymmetric Toroidal Configurations*

For toroidal magnetic field plasma confinement systems with two magnetic field components (toroidal, poloidal) a tremendous simplication occurs when the system is symmetric in the toroidal direction. Then, axisymmetric magnetic flux surfaces are guaranteed to exist and both a Clebsch and flux surface representation are available. The resulting magnetic field system is the simplest, nontrivial toroidal magnetic field system and is the basic paradigm for all types of toroidal magnetic confinement systems.

In this section we develop the commonly used axisymmetric toroidal magnetic field descriptions and coordinate systems in general — without using a large aspect ratio expansion. We also show the relationship of the descriptions and coordinates to the large aspect ratio tokamak and screw pinch models. At the end of the section we discuss how the general axisymmetric toroidal model can be used to describe other axisymmetric toroidal magnetic configurations.

The geometry we consider for an axisymmetric tokamak is shown in Fig. 3.7. Since the toroidal magnetic field is in the direction of axisymmetry (ζ) and $\boldsymbol{\nabla}\zeta = \hat{\mathbf{e}}_\zeta/R$ in which R is the major radius, it can be written as

$$\mathbf{B}_{\rm tor} \;=\; B_{\rm tor}\hat{\mathbf{e}}_\zeta \;=\; R\,B_{\rm tor}\boldsymbol{\nabla}\zeta \;\equiv\; I\,\boldsymbol{\nabla}\zeta, \quad \text{toroidal magnetic field,} \tag{3.90}$$

in which we have defined

$$I \;\equiv\; R\,B_{\rm tor}, \quad \text{toroidal field function.} \tag{3.91}$$

Because of the axisymmetry, I must be independent of ζ: $\partial I/\partial\zeta = 0$. The toroidal field function I can be related to the current flowing in the poloidal (θ) direction. The poloidal curent flowing through a disk of (major) radius R that

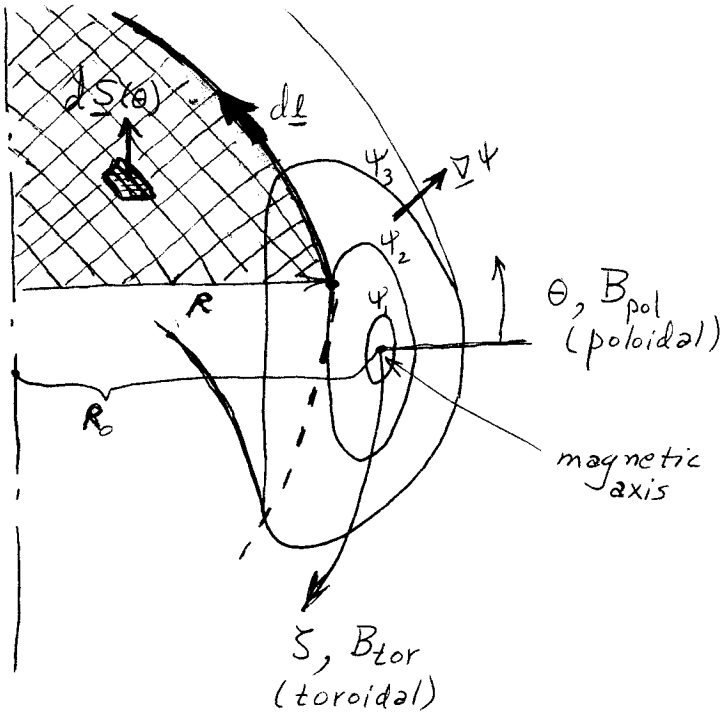

Figure 3.7: Axismmetric tokamak coordinates (ψ, θ, ζ) and geometry for calculating the poloidal current and magnetic flux.

is perpendicular to the axis of symmetry, as shown in Fig. 3.7, is given, using Ampere's magnetostatic law $\boldsymbol{\nabla}\times\mathbf{B} = \mu_0\mathbf{J}$ and Stokes' theorem (**??**), by

$$\begin{aligned} I_{\rm pol} \equiv \iint_S d\mathbf{S}(\theta)\cdot\mathbf{J} \;&=\; \oint_C d\boldsymbol{\ell}\cdot\mathbf{B}/\mu_0 \;=\; -\int_0^{2\pi} R\,d\zeta\, B_{\rm tor}/\mu_0 \\ &=\; -\,(2\pi/\mu_0)\,RB_{\rm tor} \;=\; -\,(2\pi/\mu_0)\,I. \end{aligned} \tag{3.92}$$

Here, the minus sign occurs because the differential line element on the curve C along the perimeter of the surface S is in the $-\zeta$ direction: $d\boldsymbol{\ell} \equiv -\,\hat{\mathbf{e}}_\zeta d\zeta$. Thus, the toroidal field function I represents the poloidal current $I_{\rm pol}$ flowing in the plasma and coils outside it. For isotropic pressure plasmas $I = I(\psi)$, i.e., $\partial I/\partial\theta = 0$.

In the limit of no current flowing in the plasma, the toroidal field function I is constant and determined by the poloidal currents flowing in the toroidal magnetic field coils around the plasma. Then, as can be inferred [see (**??**)] from the magnetic field caused by current flowing in an infinite wire on the symmetry axis ($R = 0$), the vacuum toroidal magnetic field strength decreases as one over

the major radius R:

$$B_{\rm tor} = I_0/R = B_0 R_0/R, \quad \text{vacuum toroidal magnetic field strength,} \tag{3.93}$$

in which B_0 and R_0 are the magnetic field strength and major radius at the magnetic axis.

Next, we develop a form for the poloidal magnetic field $\mathbf{B}_{\rm pol}$. Using the magnetic flux definition in (3.36) and taking account of the axisymmetry in the toroidal (ζ) direction, the poloidal magnetic flux can be written in terms of the toroidal component of the vector potential ($A_{\rm tor} \equiv \hat{\mathbf{e}}_\zeta \cdot \mathbf{A} = R\,\boldsymbol{\nabla}\zeta \cdot \mathbf{A}$):

$$\Psi_{\rm pol} \,=\, \iint_S d\mathbf{S}(\theta)\cdot\mathbf{B} \,=\, \oint_C d\boldsymbol{\ell}\cdot\mathbf{A} \,=\, -\int_0^{2\pi} R\,d\zeta\, A_{\rm tor} \,=\, -\,2\pi R\, A_{\rm tor}. \tag{3.94}$$

For simplicity in the final tokamak magnetic field represention, it is convenient to define a normalized poloidal magnetic flux function:

$$\boxed{\psi \,\equiv\, \Psi_{\rm pol}/2\pi \,=\, -\,R\,A_{\rm tor}, \quad \text{poloidal flux function.}} \tag{3.95}$$

Since by definition $\partial\psi/\partial\zeta = 0$, the poloidal flux fuction ψ is independent of the toroidal angle ζ but in general depends on the cylindrical-like coordinates in a ζ = constant plane: $\psi = \psi(r,\theta)$. In terms of this poloidal flux function the toroidal component of the vector potential can be written $A_{\rm tor} = -\,\psi/R$, or vectorially as $\mathbf{A}_{\rm tor} = -(\psi/R)\,\hat{\mathbf{e}}_\zeta = -\psi\boldsymbol{\nabla}\zeta$. Thus, using (3.40), the magnetic field component produced by this magnetic flux becomes

$$\mathbf{B}_{\rm pol} \,=\, \boldsymbol{\nabla}\times\mathbf{A}_{\rm tor} \,=\, \boldsymbol{\nabla}\zeta\times\boldsymbol{\nabla}\psi, \quad \text{poloidal magnetic field.} \tag{3.96}$$

The strength of the poloidal magnetic field is

$$B_{\rm pol} \,=\, |\boldsymbol{\nabla}\zeta\times\boldsymbol{\nabla}\psi| \,=\, |\boldsymbol{\nabla}\psi|/R, \quad \text{poloidal magnetic field strength,} \tag{3.97}$$

which shows that $|\boldsymbol{\nabla}\psi| = RB_{\rm pol}$. The magnetic axis of the tokamak is defined to be where $\mathbf{B}_{\rm pol} = \mathbf{0}$ and hence $\boldsymbol{\nabla}\psi = \mathbf{0}$.

Adding the two components of the magnetic field, the total magnetic field becomes simply

$$\boxed{\mathbf{B} \,=\, \mathbf{B}_{\rm tor} + \mathbf{B}_{\rm pol} \,=\, I\boldsymbol{\nabla}\zeta + \boldsymbol{\nabla}\zeta\times\boldsymbol{\nabla}\psi, \quad \text{axisymmetric magnetic field.}} \tag{3.98}$$

While this form is quite compact, it is unfortunately in neither a Clebsch form nor a two component magnetic flux form. Also, it is not written in terms of straight-field-line coordinates, and it is a mixed covariant and contravariant form — see Section D.8. Nonetheless, because this representation is compact and rigorously valid it is heavily used in analyses of axisymmetric toroidal and in particular tokamak plasmas.

Since by axisymmetry the poloidal flux function must be independent of the toroidal angle (i.e., $\partial\psi/\partial\zeta = 0$), taking the dot product of $\mathbf{B}$ with $\boldsymbol{\nabla}\psi$ we obtain

$$\mathbf{B}\cdot\boldsymbol{\nabla}\psi \,=\, (\mathbf{B}_{\rm tor} + \mathbf{B}_{\rm pol})\cdot\boldsymbol{\nabla}\psi \,=\, I\boldsymbol{\nabla}\zeta\cdot\boldsymbol{\nabla}\psi + \boldsymbol{\nabla}\zeta\times\boldsymbol{\nabla}\psi\cdot\boldsymbol{\nabla}\psi \,=\, 0. \tag{3.99}$$

Thus, the poloidal flux function ψ satisfies the flux surface condition (3.37); hence, magnetic field lines in axisymmetric toroidal systems lie on ψ = constant surfaces and ψ will be a convenient magnetic flux surface label and radial coordinate. Note that, by construction and because of axisymmetry, ψ is a suitable magnetic flux function for both the toroidal and poloidal magnetic fields. Thus, we can develop a combined magnetic fluxes and Clebsch magnetic field representation like (3.45) based on it.

So far we have identified two useful curvilinear coordinates for describing the tokamak magnetic field: the axisymmetry angle ζ for the toroidal angle and the poloidal magnetic flux function ψ for the "radial" variable. Next, we need to identify a useful poloidal angle variable. We would like to have a poloidal angle coordinate in which magnetic field lines are straight. Thus, we would like a poloidal angle such that the magnetic field representation could be put in the combined Clebsch and magnetic flux representation given by (3.45), with $\iota/2\pi$ replaced by $1/q$ and $\Psi_{\rm tor}/2\pi$ replaced by ψ for a tokamak representation.

In order to put the tokamak magnetic field (3.98) in the form of (3.45), the toroidal magnetic field (3.90) must be put into the straight-field-line form

$$\mathbf{B}_{\rm tor} = \boldsymbol{\nabla}\psi\times\boldsymbol{\nabla}(q\Theta) \quad \Longrightarrow \quad \mathbf{B} = \boldsymbol{\nabla}\psi\times\boldsymbol{\nabla}(q\Theta - \zeta) \tag{3.100}$$

in which $\theta_{\rm f} \to \Theta$ (tokamak convention) is the desired straight field line poloidal angle. Taking the dot product of the two forms of $\mathbf{B}_{\rm tor}$ given in (3.90) and (3.100) with $\boldsymbol{\nabla}\zeta$ and equating them, we obtain

$$\begin{aligned} \mathbf{B}_{\rm tor}\cdot\boldsymbol{\nabla}\zeta \;&=\; I\boldsymbol{\nabla}\zeta\cdot\boldsymbol{\nabla}\zeta = I/R^2 \\ &=\; \boldsymbol{\nabla}\psi\times\boldsymbol{\nabla}(q\Theta)\cdot\boldsymbol{\nabla}\zeta \;=\; q\,(\boldsymbol{\nabla}\zeta\times\boldsymbol{\nabla}\psi)\cdot\boldsymbol{\nabla}\Theta \;=\; q\,\mathbf{B}_{\rm pol}\cdot\boldsymbol{\nabla}\Theta \end{aligned} \tag{3.101}$$

in which we have used $\boldsymbol{\nabla}q\times\boldsymbol{\nabla}\psi = \mathbf{0}$ [because q is only a function of ψ — see (3.105) below] and the order of the vector operations has been rearranged using (**??**) and (**??**). Equating the results on the two lines of (3.101), we find

$$\mathbf{B}_{\rm pol}\cdot\boldsymbol{\nabla}\Theta \;=\; I/qR^2 \;=\; \mathbf{B}\cdot\boldsymbol{\nabla}\Theta, \tag{3.102}$$

where the last equality follows from the fact that since by axisymmetry the angle Θ must be independent of ζ, $\mathbf{B}_{\rm tor}\cdot\boldsymbol{\nabla}\Theta = 0$; thus, $\mathbf{B}\cdot\boldsymbol{\nabla}\Theta = \mathbf{B}_{\rm pol}\cdot\boldsymbol{\nabla}\Theta$. Defining a differential length $d\ell_{\rm pol}$ in the poloidal direction on a magnetic flux surface, the last form of (3.101) yields

$$\frac{\partial\Theta}{\partial\ell_{\rm pol}} \;=\; \frac{1}{\mathbf{B}\cdot\boldsymbol{\nabla}\ell_{\rm pol}}\,\frac{I}{qR^2} \quad \Longrightarrow \quad \Theta \;=\; \frac{1}{q}\int^{\ell_{\rm pol}}\frac{d\ell_{\rm pol}}{\mathbf{B}\cdot\boldsymbol{\nabla}\ell_{\rm pol}}\,\frac{I}{R^2}, \tag{3.103}$$

in which the integration is to be performed at constant ψ, ζ. The poloidal length variable $\ell_{\rm pol}$ can be defined in terms of the ordinary cylindrical angle θ about the magnetic axis. Taking the dot product of the field line equation (3.28) with $\boldsymbol{\nabla}\theta$ and $\boldsymbol{\nabla}\ell_{\rm pol}$, we find that the poloidal length variable is related to the cylindrical angle by

$$\frac{d\mathbf{x}\cdot\boldsymbol{\nabla}\theta}{d\ell} = \frac{\mathbf{B}\cdot\boldsymbol{\nabla}\theta}{B}, \quad \frac{d\mathbf{x}\cdot\boldsymbol{\nabla}\ell_{\rm pol}}{d\ell} = \frac{\mathbf{B}\cdot\boldsymbol{\nabla}\ell_{\rm pol}}{B} \quad \Longrightarrow \quad \frac{d\theta}{\mathbf{B}\cdot\boldsymbol{\nabla}\theta} = \frac{d\ell_{\rm pol}}{\mathbf{B}\cdot\boldsymbol{\nabla}\ell_{\rm pol}}. \tag{3.104}$$

Integrating the last form of (3.103) over one complete poloidal traversal of the flux surface, which we define to be $\Theta = 2\pi$, we obtain an expression for the toroidal winding number:

$$q(\psi) \;=\; \frac{1}{2\pi}\oint \frac{d\ell_{\rm pol}}{\mathbf{B}\cdot\boldsymbol{\nabla}\ell_{\rm pol}}\,\frac{I}{R^2} \;=\; \frac{1}{2\pi}\oint \frac{d\theta}{\mathbf{B}\cdot\boldsymbol{\nabla}\theta}\,\frac{I}{R^2}$$

or,

$$\boxed{q(\psi) \;=\; \frac{1}{2\pi}\oint d\theta\,\frac{\mathbf{B}\cdot\boldsymbol{\nabla}\zeta}{\mathbf{B}\cdot\boldsymbol{\nabla}\theta} \;\simeq\; \frac{1}{2\pi}\oint d\theta\,\frac{rB_{\rm tor}}{RB_{\rm pol}} \;\simeq\; \frac{rB_{\rm tor}}{RB_{\rm pol}}[1+\mathcal{O}\{\epsilon^2\}].} \quad (3.105)$$

Here, we have used $I/R^2 = \mathbf{B}\cdot\boldsymbol{\nabla}\zeta$ from (3.101) and indicated in the approximate equalities (here and below) the forms that result in the large aspect ratio limit ($\epsilon << 1$). Note that the lowest order, approximate form for q agrees with the screw pinch model result (3.74).

The toroidal winding number q may be an integer or the ratio of two integers (e.g., $q = m/n$); then, a magnetic field line on that surface would close on itself after an integer number of poloidal (n) and toroidal (m) transits around the torus — see (3.74) and Fig. 3.8. Such a surface is called a rational surface. All magnetic field lines on a rational surface rotate with the same rotational transform ι, running forever parallel to adjacent field lines on the flux surface; hence, they sample only a given field line on the flux surface. On the other hand, if q is not the ratio of two integers, then the flux surface is called irrational. Thus, we define (see Fig. 3.8)

$$\boxed{\begin{array}{ll} q(\psi) = m/n, & \text{rational flux surface,} \\ q(\psi) \neq m/n, & \text{irrational flux surface,} \end{array}} \quad (3.106)$$

in which m, n are integers. Magnetic field lines on an irrational flux surface do not close on themselves; however, if they are followed long enough, they fill the entire flux surface. This is called ergodic behavior since all points on the surface are then equally sampled — at least statistically in an asymptotic limit. Note that the vast majority of flux surfaces are irrational; they form a dense set. Rational surfaces are "infrequent," separated radially (i.e., in ψ) and of measure zero. Nonetheless, they are very important in magnetized toroidal plasmas because physical processes taking place on adjacent rational field lines are mostly isolated from each other, and because they are degenerate field lines that are especially vulnerable to resonant nonaxisymmetric perturbations that can produce magnetic island structures like those discussed in Section 3.3.

An explicit expression for Θ will now be obtained. Using the rigorous form of the definition of q in (3.105) and defining Θ like the simple geometric angle θ to be zero on the outer midplane of the torus, we can develop from (3.104) explicit expressions for the straight-field-line poloidal angle:

$$\Theta \;\equiv\; \frac{1}{q}\int_0^{\ell_\theta} \frac{d\ell_\theta}{\mathbf{B}\cdot\boldsymbol{\nabla}\ell_\theta}\,\frac{I}{R^2} \;=\; \frac{1}{q}\int_0^{\theta} \frac{d\theta}{\mathbf{B}\cdot\boldsymbol{\nabla}\theta}\,\frac{I}{R^2} \;=\; \frac{1}{q}\int_0^{\theta} d\theta\,\frac{\mathbf{B}\cdot\boldsymbol{\nabla}\zeta}{\mathbf{B}\cdot\boldsymbol{\nabla}\theta}. \quad (3.107)$$

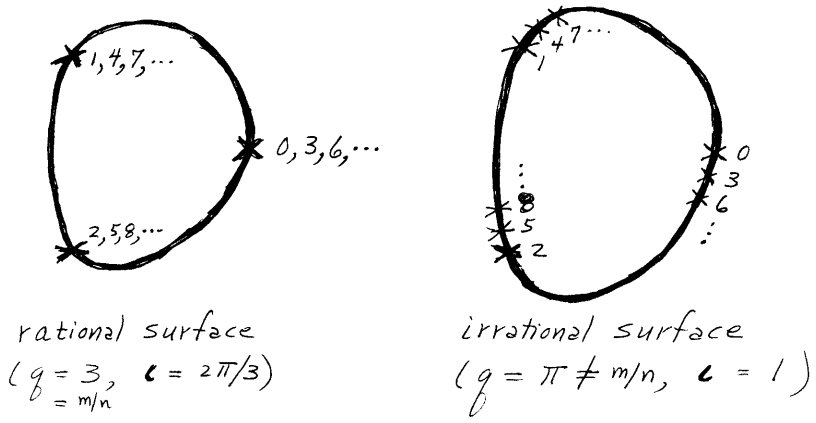

Figure 3.8: "Puncture plots" of magnetic field lines in a ζ = constant plane on a magnetic flux surface in an axisymmetric torus. The numbers listed indicate the number of toroidal transits executed by a field line. On rational surfaces field lines retrace the same trajectory after m toroidal transits whereas on an irrational surface a single field line is ergodic and (eventually) samples the entire surface.

It can be shown using steps like the last few ones in (3.105) that, to lowest order in a large aspect ratio expansion (e.g., near the magnetic axis), the straight field line coordinate Θ is equal to the local cylindrical coordinate θ:

$$\Theta \;=\; \theta - \mathcal{O}\{\epsilon \sin\theta\}. \tag{3.108}$$

The order ϵ sinusoidal variations of Θ with θ depend on the currents flowing in the plasma; their evaluation will be deferred until Chapter 20 where we use the macroscopic force balance equations in a finite-pressure tokamak plasma to determine the currents in a tokamak plasma and the shape of the $\psi(\mathbf{x})$ surfaces.

As can be seen from Fig. 3.1d, the magnetic field in a tokamak has parallel and perpendicular gradients, curvature (both normal and geodesic), and local torsion and shear that are not constant along the magnetic field. Below, we will give general expressions for each of these properties both in general, and also in their lowest order forms in a large aspect ratio ($\epsilon << 1$), low plasma pressure expansion. To lowest (zeroth) order the magnetic flux surfaces become circles about the magnetic axis. (To first order in ϵ the flux surfaces are still circles, but their centers are shifted outward slightly in major radius — see Section 20.4.) Thus, to lowest order we will use the r, θ, z coordinates of a cylinder whose z axis lies on the magnetic axis of the tokamak, of a type shown in Fig. 3.1d. To lowest order the model will mostly reduce to the screw pinch model discussed in the preceding section — compare Fig. 3.5 with Fig. 3.7.

The major radius R to any point in the plasma will be given in terms of the

major radius of the magnetic axis (R_0) and the local cylindrical coordinates by

$$R \,=\, R(\psi,\Theta) \,\simeq\, R_0\,[\,1+\epsilon\cos\theta+\mathcal{O}\{\epsilon^2\}]. \tag{3.109}$$

Using this approximate representation in the equation for the vacuum magnetic field strength variation with R given in (3.93) and the fact that in our tokamak model $B \simeq B_{\rm tor}\,[\,1+\mathcal{O}\{\epsilon^2/q^2\}]$, we obtain

$$\boxed{B \,=\, B(\psi,\Theta) \,\simeq\, B(r,\theta) \,\simeq\, B_0\,[\,1-\epsilon\cos\theta+\mathcal{O}\{\epsilon^2\}],\quad \text{tokamak field strength.}} \tag{3.110}$$

The magnetic field strength in a tokamak varies approximately sinusoidally along a helical magnetic field line from its minimum on the outside ($\theta=0$ where $B_{\rm min}/B_0 \simeq 1-\epsilon$) to its maximum on the inside ($\theta=\pi$ where $B_{\rm max}/B_0 \simeq 1+\epsilon$) of the torus. Thus, it can be represented by the sinusoidal model in (3.6) using $\ell \to R_0 q\,\theta$ and $L_\ell \to 2\pi R_0 q$. The magnitude of the variation along a magnetic field line is usually small: $\Delta B \equiv B_{\rm max}-B_{\rm min} \simeq 2\epsilon B_0 << B_0$. Hence, the magnetic mirror ratio defined in (3.7) is usually only slightly greater than unity: $R_m \equiv B_{\rm max}/B_{\rm min} \simeq 1+2\epsilon$. In summary, the variation of the magnetic field strength along field lines in large aspect ratio tokamaks can be modeled by (3.6) with

$$B_{\rm min} \simeq (1-\epsilon)B_0,\quad \Delta B \simeq 2\epsilon B_0,\quad \ell \to R_0 q\,\theta,\quad L_\ell \to 2\pi R_0 q,$$
$$\text{tokamak } B_{\rm sin} \text{ model parameters.} \tag{3.111}$$

To calculate the perpendicular gradient, curvature and shear in the tokamak magnetic field we need to explicitly relate the tokamak magnetic flux system coordinates ψ,Θ,ζ, which are unfortunately not orthogonal ($\boldsymbol{\nabla}\Theta\cdot\boldsymbol{\nabla}\psi \neq 0$), to the local cylindrical coordinates (r,θ,z) about the magnetic axis:

$$\boldsymbol{\nabla}\psi \,\simeq\, B_{\rm pol}R\,\boldsymbol{\nabla}r \,\simeq\, B_{\rm pol}R_0\,\hat{\mathbf{e}}_{\rm r},\quad \psi(r) \,\simeq\, \int_0^r dr\,B_{\rm pol}R_0, \tag{3.112}$$

$$\boldsymbol{\nabla}\Theta \,\simeq\, \boldsymbol{\nabla}\theta \,\simeq\, \frac{\hat{\mathbf{e}}_\theta}{r},\quad \mathbf{B}\cdot\boldsymbol{\nabla}\Theta \,=\, \frac{I}{qR^2} \,\simeq\, \frac{B_{\rm pol}}{r} \,\simeq\, \frac{B_0}{R_0 q}, \tag{3.113}$$

$$\boldsymbol{\nabla}\zeta \,=\, \frac{\hat{\mathbf{e}}_\zeta}{R} \,\simeq\, \frac{\hat{\mathbf{e}}_\zeta}{R_0}\,[\,1-\epsilon\cos\theta+\mathcal{O}\{\epsilon^2\}]. \tag{3.114}$$

The poloidal magnetic field strength oscillates slightly with poloidal angle:

$$B_{\rm pol} \,\equiv\, |\boldsymbol{\nabla}\psi|/R \,\simeq\, (\epsilon/q)B_0\,[\,1+\mathcal{O}\{\epsilon\cos\theta\}]. \tag{3.115}$$

In calculating gradients of various quantities in tokamak system coordinates, we just use chain rule differentiation:

$$\frac{\boldsymbol{\nabla}_\perp B}{B} \,=\, \frac{1}{B}\left(\boldsymbol{\nabla}\psi\frac{\partial B}{\partial\psi}+\boldsymbol{\nabla}_\perp\Theta\frac{\partial B}{\partial\Theta}\right) \,\simeq\, \frac{1}{R_0}\,[\,-\hat{\mathbf{e}}_r\,\cos\theta+\hat{\mathbf{e}}_\theta\sin\theta+\mathcal{O}\{\epsilon\}\,]\,. \tag{3.116}$$

in which we have used (3.93) and $\partial/\partial\zeta$ terms vanish by axisymmetry. In a tokamak with low plasma pressure and hence a small poloidal current (see Chapter 20) the $\mathbf{J}\times\mathbf{B}$ contribution to the curvature is small. Thus, using (3.20) the curvature is given by

$$\boldsymbol{\kappa} = \frac{\boldsymbol{\nabla}_{\perp B}}{B} + \mu_0 \frac{\mathbf{J}\times\mathbf{B}}{B^2} \simeq \frac{1}{B}\left(\boldsymbol{\nabla}\psi\,\frac{\partial B}{\partial\psi} + \boldsymbol{\nabla}_\perp\Theta\,\frac{\partial B}{\partial\Theta}\right)$$
$$\simeq \frac{1}{R_0}\left[-\hat{\mathbf{e}}_r\cos\theta + \hat{\mathbf{e}}_\theta\sin\theta + \mathcal{O}\{\epsilon\}\right], \quad \text{tokamak curvature vector.} \quad (3.117)$$

To this lowest order the curvature is simply the toroidal curvature of the system. Note that a tokamak has both normal (perpendicular to the flux surface, $\kappa_{\text{N}} \simeq \kappa_r = -\cos\theta/R_0$) and geodesic (within the flux surface, $\kappa_{\text{B}} \simeq \kappa_\theta = \sin\theta/R_0$) curvature — see Section D.6. Note further that, because of the inclusion of toroidicity effects, the tokamak curvature is one order in ϵ larger than that in the screw pinch model (3.84); however, its sign oscillates with the poloidal angle θ and its average is of the same order as the curvature in the screw pinch model. To determine the $\mathcal{O}\{\epsilon\}$ terms in (3.117) we need to take account of the plasma pressure and current profiles in the tokamak — see Chapter 20.

Using a number of vector identities and other manipulations (see Problem 3.29), it can be shown that the normal torsion in a tokamak can be written as

$$\tau_{\text{N}} = \frac{I\,|\boldsymbol{\nabla}\psi|}{B^2 R}(\mathbf{B}\cdot\boldsymbol{\nabla}\Theta)\left[\frac{\partial}{\partial\psi}\left(\frac{qR|\boldsymbol{\nabla}\psi|}{I}\right) + \frac{\partial}{\partial\Theta}\left(\frac{qR|\boldsymbol{\nabla}\psi|}{I}\frac{\partial\Theta}{\partial\psi}\right)\right]$$
$$\simeq \frac{1}{R_0 q}\left[1 + \mathcal{O}\{\epsilon\cos\theta\}\right], \quad \text{tokamak local torsion,} \quad (3.118)$$

which to the lowest order is the same as in the screw pinch model — see (3.81). Similarly, the magnetic shear in a tokamak becomes (see Problem 3.31):

$$\varsigma_y = -\frac{|\boldsymbol{\nabla}\psi|^2}{B^2}(\mathbf{B}\cdot\boldsymbol{\nabla})\left[\frac{\partial}{\partial\psi}(q\Theta)\right] = -\frac{|\boldsymbol{\nabla}\psi|^2}{B^2}(\mathbf{B}\cdot\boldsymbol{\nabla}\Theta)\left[\frac{dq}{d\psi} + q\frac{\partial}{\partial\Theta}\left(\frac{\partial\Theta}{\partial\psi}\right)\right]$$
$$\simeq -\frac{1+\mathcal{O}(\epsilon\cos\theta)}{R_0 q}\left[s - \mathcal{O}\{\epsilon\cos\theta\}\right], \quad \text{tokamak local shear,} \quad (3.119)$$

which again to lowest order is the same as in the screw pinch model — see (3.86). [The convention in the tokamak literature is to reverse the sign of the shear — so that it is positive for normal tokamaks in which q increases with radius (see Fig. 3.6).] Note that both the local torsion and local shear have order ϵ sinsoidal variations along a magnetic field line as it moves from the outside to inside of the torus — but their averages over a magnetic flux surface (i.e., over θ) are approximately given by their respective values in the screw pinch model. Again, to obtain the next order (ϵ) terms correctly we need to take account of plasma currents and pressures, which we defer until Chapter 20.

In this section we have developed the magnetic field representation and properties of axisymmetric toroidal magnetic field systems in general, and then indicated the lowest order results in the large aspect ratio expansion ($\epsilon \equiv r/R_0 =$

$1/A << 1$) after an approximate equality sign ($\simeq$). While the discussion has focused on the tokamak magnetic field structure, the general development applies to any axisymmetric toroidal system. Thus, it applies to spherical tokamaks [very low aspect ratio ($A \sim 1.1$–1.5) tokamaks], spheromaks [effectively unity aspect ratio tokamaks without toroidal field coils] and reversed field pinches [effectively tokamaks with very low $q \sim \epsilon << 1$]. For spherical tokamaks and spheromaks the full generality of the magnetic flux coordinates must be used because a large aspect ratio expansion is invalid — except for small radius flux surfaces near the magnetic axis where a large aspect ratio expansion can be used. As indicated at the end of the preceding section, the general screw pinch model represents reversed field pinches except for the purely toroidal effects (variation of B from the outer to inner edge of the torus and toroidal curvature of field lines). These latter effects are included in the general magnetic flux model developed in this section. In summary, the general magnetic flux surface model developed in this section is appropriate for describing all types of axisymmetric toroidal magnetic field configurations — tokamaks, reversed field pinches, spherical tokamaks, and spheromaks.

3.7 Local Expansion of a Magnetic Field+

In order to develop a comprehensive picture of all the possible first derivative properties of a magnetic field, in this section we carry out a formal Taylor series expansion of the magnetic induction vector field $\mathbf{B}(\mathbf{x})$. The expansion will be carried out at an arbitrary point in the magnetic configuration where the origin of a local Cartesian coordinate system will be placed. Thus, our local Taylor series expansion (subscript le) becomes

$$\mathbf{B}_{\rm le}(\mathbf{x}) \;=\; \mathbf{B}_0 + \mathbf{x}\cdot\boldsymbol{\nabla}\mathbf{B}_0 + \ldots\,, \tag{3.120}$$

in which $\mathbf{B}_0$ is the magnetic induction field at the chosen point, $\mathbf{x}$ is the vector distance from this point, and $\boldsymbol{\nabla}\mathbf{B}_0$ represents the evaluation of the tensor $\boldsymbol{\nabla}\mathbf{B}$ at this point. The second and higher order terms in (3.120) will be neglected since we are interested here only in the local properties of non-pathological magnetic fields for which the first derivatives provide a sufficient description.

This section uses a number of vector differentiation identities and seeks to connect the local magnetic field derivatives to the common definitions of most of these properties for arbitrary vector fields. These subjects are summarized briefly in Appendix D, and in particular in the Section D.6. Readers are encouraged to read the relevant sections in Appendix D in conjunction with this section.

As usual we decompose the magnetic induction field $\mathbf{B}(\mathbf{x})$ into its vector direction and scalar magnitude components at any spatial point $\mathbf{x}$ by writing

$$\mathbf{B}(\mathbf{x}) \;=\; B\,\hat{\mathbf{b}} \;=\; B(\mathbf{x})\,\hat{\mathbf{b}}(\mathbf{x}), \tag{3.121}$$

in which

$$B(\mathbf{x}) \equiv |\mathbf{B}(\mathbf{x})| = \sqrt{\mathbf{B}\cdot\mathbf{B}}, \quad \text{magnetic field strength,} \tag{3.122}$$
$$\hat{\mathbf{b}}(\mathbf{x}) \equiv \mathbf{B}(\mathbf{x})/B(\mathbf{x}) = \mathbf{B}/B, \quad \text{unit vector along } \mathbf{B}(\mathbf{x}). \tag{3.123}$$

Using this decomposition, we can write the tensor $\boldsymbol{\nabla}\mathbf{B}_0$ as

$$\boldsymbol{\nabla}\mathbf{B}_0 \equiv (\boldsymbol{\nabla}B\,\hat{\mathbf{b}})_0 = \hat{\mathbf{b}}_0\boldsymbol{\nabla}B_0 + B_0\boldsymbol{\nabla}\hat{\mathbf{b}}_0, \tag{3.124}$$

in which $\hat{\mathbf{b}}_0$ is the unit vector $\hat{\mathbf{b}}$ evaluated at the origin (point of interest) and $\boldsymbol{\nabla}B_0$, $\boldsymbol{\nabla}\hat{\mathbf{b}}_0$ are $\boldsymbol{\nabla}B$, $\boldsymbol{\nabla}\hat{\mathbf{b}}$ evaluated at this same point.

To work out the various components of the $\boldsymbol{\nabla}\hat{\mathbf{b}}$ and hence $\boldsymbol{\nabla}\mathbf{B}$ tensors we can use a local Cartesian coordinate system whose z axis is aligned along $\hat{\mathbf{b}}$ at $\mathbf{x} = (0,0,0)$ (i.e., $\hat{\mathbf{b}}_0$) and which has its x axis in a particular direction perpendicular to $\hat{\mathbf{b}}_0$, which we will specify later. Thus, the orthonormal triad of unit vectors characterizing this local coordinate system will be $\hat{\mathbf{e}}_z = \hat{\mathbf{b}}_0$, $\hat{\mathbf{e}}_x$, $\hat{\mathbf{e}}_y \equiv \hat{\mathbf{b}}_0\times\hat{\mathbf{e}}_x$. For notational simplicity, in what follows we omit the subscript zero on the magnetic field unit vector $\hat{\mathbf{b}}$.

Consider first the components locally parallel to the magnetic field:

$$\begin{aligned}
(\boldsymbol{\nabla}\hat{\mathbf{b}})_{zz} &\equiv \hat{\mathbf{b}}\cdot(\hat{\mathbf{b}}\cdot\boldsymbol{\nabla})\hat{\mathbf{b}} = -\,\hat{\mathbf{b}}\cdot\hat{\mathbf{b}}\times(\boldsymbol{\nabla}\times\hat{\mathbf{b}}) = 0,\\
(\boldsymbol{\nabla}\hat{\mathbf{b}})_{zx} &\equiv [(\hat{\mathbf{b}}\cdot\boldsymbol{\nabla})\hat{\mathbf{b}}]\cdot\hat{\mathbf{e}}_x = \hat{\mathbf{e}}_x\cdot(\hat{\mathbf{b}}\cdot\boldsymbol{\nabla})\hat{\mathbf{b}} \neq 0,\\
(\boldsymbol{\nabla}\hat{\mathbf{b}})_{zy} &\equiv [(\hat{\mathbf{b}}\cdot\boldsymbol{\nabla})\hat{\mathbf{b}}]\cdot\hat{\mathbf{e}}_y = \hat{\mathbf{e}}_y\cdot(\hat{\mathbf{b}}\cdot\boldsymbol{\nabla})\hat{\mathbf{b}} \neq 0,\\
(\boldsymbol{\nabla}\hat{\mathbf{b}})_{xz} &\equiv \hat{\mathbf{b}}\cdot(\hat{\mathbf{e}}_x\cdot\boldsymbol{\nabla})\hat{\mathbf{b}} = \tfrac{1}{2}(\hat{\mathbf{e}}_x\cdot\boldsymbol{\nabla})(\hat{\mathbf{b}}\cdot\hat{\mathbf{b}}) = 0,\\
(\boldsymbol{\nabla}\hat{\mathbf{b}})_{yz} &\equiv \hat{\mathbf{b}}\cdot(\hat{\mathbf{e}}_y\cdot\boldsymbol{\nabla})\hat{\mathbf{b}} = \tfrac{1}{2}(\hat{\mathbf{e}}_y\cdot\boldsymbol{\nabla})(\hat{\mathbf{b}}\cdot\hat{\mathbf{b}}) = 0,
\end{aligned} \tag{3.125}$$

in which we have used the fact that since $\hat{\mathbf{b}}$ is a unit vector, we have $\hat{\mathbf{b}}\cdot\hat{\mathbf{b}} = 1$, and the vector identity,

$$\frac{1}{2}\boldsymbol{\nabla}(\hat{\mathbf{b}}\cdot\hat{\mathbf{b}}) = \mathbf{0} = \hat{\mathbf{b}}\times(\boldsymbol{\nabla}\times\hat{\mathbf{b}}) + (\hat{\mathbf{b}}\cdot\boldsymbol{\nabla})\hat{\mathbf{b}}. \tag{3.126}$$

For the components locally perpendicular to the magnetic field we have

$$\begin{aligned}
(\boldsymbol{\nabla}\hat{\mathbf{b}})_{xx} &\equiv \hat{\mathbf{e}}_x\cdot(\hat{\mathbf{e}}_x\cdot\boldsymbol{\nabla})\hat{\mathbf{b}},\\
(\boldsymbol{\nabla}\hat{\mathbf{b}})_{yy} &\equiv \hat{\mathbf{e}}_y\cdot(\hat{\mathbf{e}}_y\cdot\boldsymbol{\nabla})\hat{\mathbf{b}},\\
(\boldsymbol{\nabla}\hat{\mathbf{b}})_{xy} &\equiv \hat{\mathbf{e}}_y\cdot(\hat{\mathbf{e}}_x\cdot\boldsymbol{\nabla})\hat{\mathbf{b}} = +\,\hat{\mathbf{e}}_y\cdot\boldsymbol{\nabla}\times\hat{\mathbf{e}}_y - \hat{\mathbf{e}}_x\cdot(\hat{\mathbf{b}}\cdot\boldsymbol{\nabla})\hat{\mathbf{e}}_y,\\
(\boldsymbol{\nabla}\hat{\mathbf{b}})_{yx} &\equiv \hat{\mathbf{e}}_x\cdot(\hat{\mathbf{e}}_y\cdot\boldsymbol{\nabla})\hat{\mathbf{b}} = -\,\hat{\mathbf{e}}_x\cdot\boldsymbol{\nabla}\times\hat{\mathbf{e}}_x + \hat{\mathbf{e}}_x\cdot(\hat{\mathbf{b}}\cdot\boldsymbol{\nabla})\hat{\mathbf{e}}_y,
\end{aligned} \tag{3.127}$$

in which we have worked out the last two cross terms using vector differentiation identities (**??**) and (**??**) as follows:

$$\begin{aligned}
\hat{\mathbf{e}}_y\cdot(\hat{\mathbf{e}}_x\cdot\boldsymbol{\nabla})\hat{\mathbf{b}} &= \hat{\mathbf{e}}_y\cdot[-\boldsymbol{\nabla}\times(\hat{\mathbf{e}}_x\times\hat{\mathbf{b}}) + \hat{\mathbf{e}}_x(\boldsymbol{\nabla}\cdot\hat{\mathbf{b}}) - \hat{\mathbf{b}}\,(\boldsymbol{\nabla}\cdot\hat{\mathbf{e}}_x) + (\hat{\mathbf{b}}\cdot\boldsymbol{\nabla})\hat{\mathbf{e}}_x]\\
&= \hat{\mathbf{e}}_y\cdot\boldsymbol{\nabla}\times\hat{\mathbf{e}}_y + \hat{\mathbf{e}}_y\cdot(\hat{\mathbf{b}}\cdot\boldsymbol{\nabla})\hat{\mathbf{e}}_x = \hat{\mathbf{e}}_y\cdot\boldsymbol{\nabla}\times\hat{\mathbf{e}}_y - \hat{\mathbf{e}}_x\cdot(\hat{\mathbf{b}}\cdot\boldsymbol{\nabla})\hat{\mathbf{e}}_y,
\end{aligned} \tag{3.128}$$

and similarly for $(\boldsymbol{\nabla}\hat{\mathbf{b}})_{yx}$.

Taking the derivative of the equation along a magnetic field line given in (3.28) yields the second derivative of the field line's coordinate and hence the local curvature of the magnetic field [$d/d\ell \equiv (\hat{\mathbf{b}}\cdot\boldsymbol{\nabla})$]:

$$\boldsymbol{\kappa} \equiv \frac{d^2\hat{\mathbf{b}}(\ell)}{d\ell^2} = (\hat{\mathbf{b}}\cdot\boldsymbol{\nabla})\hat{\mathbf{b}} = -\hat{\mathbf{b}}\times(\boldsymbol{\nabla}\times\hat{\mathbf{b}}), \quad \text{curvature vector,} \tag{3.129}$$

which is perpendicular to the local magnetic field ($\hat{\mathbf{b}}\cdot\boldsymbol{\kappa} = 0$). The zx, zy components of the tensors $\boldsymbol{\nabla}\hat{\mathbf{b}}$ can be written in terms of the x, y components of the curvature vector:

$$\begin{aligned}(\boldsymbol{\nabla}\hat{\mathbf{b}})_{zx} &= \hat{\mathbf{e}}_{\mathrm{x}}\cdot(\hat{\mathbf{b}}\cdot\boldsymbol{\nabla})\hat{\mathbf{b}} = \hat{\mathbf{e}}_{\mathrm{x}}\cdot\boldsymbol{\kappa} \equiv \kappa_x,\\ (\boldsymbol{\nabla}\hat{\mathbf{b}})_{zy} &= \hat{\mathbf{e}}_{\mathrm{y}}\cdot(\hat{\mathbf{b}}\cdot\boldsymbol{\nabla})\hat{\mathbf{b}} = \hat{\mathbf{e}}_{\mathrm{y}}\cdot\boldsymbol{\kappa} \equiv \kappa_y.\end{aligned} \tag{3.130}$$

The x component of the curvature vector is the same as the κ_x in the sheared slab model given by (3.16) and (3.21). From geometrical considerations the radius of the curvature vector $\mathbf{R}_C$ is antiparallel to the curvature vector $\boldsymbol{\kappa}$. Hence it is given by

$$\mathbf{R}_C = -\boldsymbol{\kappa}/\kappa^2, \quad \text{or} \quad \boldsymbol{\kappa} = -\mathbf{R}_C/R_C^2, \quad \text{radius of curvature.} \tag{3.131}$$

The torsion of a vector field is by convention defined to be the negative of the parallel derivative of the binormal vector, which for our geometry is $\hat{\mathbf{b}}\times\hat{\mathbf{e}}_{\mathrm{x}} = \hat{\mathbf{e}}_{\mathrm{y}}$:

$$\boldsymbol{\tau} = -(\hat{\mathbf{b}}\cdot\boldsymbol{\nabla})(\hat{\mathbf{b}}\times\hat{\mathbf{e}}_{\mathrm{x}}) = -(\hat{\mathbf{b}}\cdot\boldsymbol{\nabla})\,\hat{\mathbf{e}}_{\mathrm{y}}, \quad \text{torsion vector.} \tag{3.132}$$

The x component of this vector is given by

$$\tau_x \equiv -\hat{\mathbf{e}}_{\mathrm{x}}\cdot(\hat{\mathbf{b}}\cdot\boldsymbol{\nabla})\hat{\mathbf{e}}_{\mathrm{y}} = \hat{\mathbf{e}}_{\mathrm{y}}\cdot(\hat{\mathbf{b}}\cdot\boldsymbol{\nabla})\hat{\mathbf{e}}_{\mathrm{x}}, \tag{3.133}$$

which is a quantity that appears in xy and yx components of the tensor $\boldsymbol{\nabla}\hat{\mathbf{b}}$. Physically, the torsion vector measures the change in direction (or twist) of the binormal $\hat{\mathbf{b}}\times\hat{\mathbf{e}}_{\mathrm{x}}$ as one moves along the magnetic field.

Shear of a vector field can be defined for the two directions perpendicular to the magnetic field by

$$\varsigma_x \equiv \hat{\mathbf{e}}_{\mathrm{x}}\cdot\boldsymbol{\nabla}\times\hat{\mathbf{e}}_{\mathrm{x}} = (\hat{\mathbf{b}}\times\hat{\mathbf{e}}_{\mathrm{y}})\cdot\boldsymbol{\nabla}\times(\hat{\mathbf{b}}\times\hat{\mathbf{e}}_{\mathrm{y}}), \quad \text{shear in surface perpendicular to } x, \tag{3.134}$$

$$\varsigma_y \equiv \hat{\mathbf{e}}_{\mathrm{y}}\cdot\boldsymbol{\nabla}\times\hat{\mathbf{e}}_{\mathrm{y}} = (\hat{\mathbf{b}}\times\hat{\mathbf{e}}_{\mathrm{x}})\cdot\boldsymbol{\nabla}\times(\hat{\mathbf{b}}\times\hat{\mathbf{e}}_{\mathrm{x}}), \quad \text{shear in surface perpendicular to } y. \tag{3.135}$$

That these quantities represent the local shear in the vector field $\mathbf{B}$ can be seen by realizing that, for example, $\hat{\mathbf{b}}\times\hat{\mathbf{e}}_{\mathrm{x}}$ represents the surface locally perpendicular to $\hat{\mathbf{e}}_{\mathrm{y}}$, $\boldsymbol{\nabla}\times(\hat{\mathbf{b}}\times\hat{\mathbf{e}}_{\mathrm{x}})$ represents the tangential motion (see Fig. **??**) or differential twisting of this surface, and $(\hat{\mathbf{b}}\times\hat{\mathbf{e}}_{\mathrm{x}})\cdot\boldsymbol{\nabla}\times(\hat{\mathbf{b}}\times\hat{\mathbf{e}}_{\mathrm{x}})$ is the component of this differential twisting in the original direction $\hat{\mathbf{e}}_{\mathrm{y}}$. Note that if $\hat{\mathbf{e}}_{\mathrm{x}}$ (or $\hat{\mathbf{e}}_{\mathrm{y}}$)

were a unit vector corresponding to a contravariant base vector $\boldsymbol{\nabla} u^i$ in a curvilinear coordinate system (see Section D.8), then $\hat{\mathbf{e}}_i = \boldsymbol{\nabla} u^i / |\boldsymbol{\nabla} u^i|$ and hence $\varsigma_i \equiv \hat{\mathbf{e}}_i \cdot \boldsymbol{\nabla} \times \hat{\mathbf{e}}_i = (\boldsymbol{\nabla} u^i \cdot \boldsymbol{\nabla} \times \boldsymbol{\nabla} u^i)/|\boldsymbol{\nabla} u^i|^2 = 0$. Thus, there is no shear in a direction described by the gradient of a scalar function (e.g., a magnetic flux function) — because the gradient of a scalar is an irrotational quantity ($\boldsymbol{\nabla} \times \boldsymbol{\nabla} f = \mathbf{0}$). The corresponding parallel "shear" $\hat{\mathbf{b}} \cdot \boldsymbol{\nabla} \times \hat{\mathbf{b}}$ (or parallel component of the vorticity in the vector field $\mathbf{B}$) can be written in terms of the x component of the torsion vector and the two perpendicular shear components as follows:

$$\varsigma_z \equiv \hat{\mathbf{b}} \cdot \boldsymbol{\nabla} \times \hat{\mathbf{b}} = 2\,\tau_x + \varsigma_x + \varsigma_y, \quad \text{parallel component of vorticity in } \mathbf{B} \text{ field.} \tag{3.136}$$

In the absence of shear, this relation is analogous to the component of rotation of a rigidly rotating fluid in its direction of flow, i.e., $\frac{1}{2}\mathbf{V} \cdot \boldsymbol{\nabla} \times \mathbf{V}$.

The xy and yx or cross components of the $\boldsymbol{\nabla}\hat{\mathbf{b}}$ tensor can be written in terms of the x, y components of the torsion and shear as follows:

$$\begin{aligned} (\boldsymbol{\nabla}\hat{\mathbf{b}})_{xy} &= \varsigma_y + \tau_x, \\ (\boldsymbol{\nabla}\hat{\mathbf{b}})_{yx} &= \varsigma_x + \tau_x. \end{aligned} \tag{3.137}$$

The divergence of the unit vector $\hat{\mathbf{b}}$ can be written as [using (**??**)]

$$\boldsymbol{\nabla} \cdot \hat{\mathbf{b}} = \hat{\mathbf{e}}_{\mathrm{x}} \cdot (\hat{\mathbf{e}}_{\mathrm{x}} \cdot \boldsymbol{\nabla})\hat{\mathbf{b}} + \hat{\mathbf{e}}_{\mathrm{y}} \cdot (\hat{\mathbf{e}}_{\mathrm{y}} \cdot \boldsymbol{\nabla})\hat{\mathbf{b}} + \overbrace{\hat{\mathbf{b}} \cdot (\hat{\mathbf{b}} \cdot \boldsymbol{\nabla})\hat{\mathbf{b}}}^{0}. \tag{3.138}$$

Thus, the xx and yy (or diagonal matrix element) components of the $\boldsymbol{\nabla}\hat{\mathbf{b}}$ tensor represent the x and y components of the divergence of the unit vector $\hat{\mathbf{b}}$. We define these divergence (δ) components of the vector field $\mathbf{B}$ as follows:

$$\begin{aligned} \delta_x &\equiv \hat{\mathbf{e}}_{\mathrm{x}} \cdot (\hat{\mathbf{e}}_{\mathrm{x}} \cdot \boldsymbol{\nabla})\hat{\mathbf{b}} = (1/B)[\hat{\mathbf{e}}_{\mathrm{x}} \cdot (\hat{\mathbf{e}}_{\mathrm{x}} \cdot \boldsymbol{\nabla})\mathbf{B}], \\ \delta_y &\equiv \hat{\mathbf{e}}_{\mathrm{y}} \cdot (\hat{\mathbf{e}}_{\mathrm{y}} \cdot \boldsymbol{\nabla})\hat{\mathbf{b}} = (1/B)[\hat{\mathbf{e}}_{\mathrm{y}} \cdot (\hat{\mathbf{e}}_{\mathrm{y}} \cdot \boldsymbol{\nabla})\mathbf{B}]. \end{aligned} \tag{3.139}$$

Collecting together the various components of the tensor $\boldsymbol{\nabla}\hat{\mathbf{b}}$ we thus find, in matrix form,

$$\boldsymbol{\nabla}\hat{\mathbf{b}} = (\hat{\mathbf{e}}_{\mathrm{x}}\ \hat{\mathbf{e}}_{\mathrm{y}}\ \hat{\mathbf{b}}) \begin{pmatrix} \delta_x & \tau_x + \varsigma_y & 0 \\ -\tau_x - \varsigma_x & \delta_y & 0 \\ \kappa_x & \kappa_y & 0 \end{pmatrix} \begin{pmatrix} \hat{\mathbf{e}}_{\mathrm{x}} \\ \hat{\mathbf{e}}_{\mathrm{y}} \\ \hat{\mathbf{b}} \end{pmatrix}. \tag{3.140}$$

Further, using this result in (3.124), we find that the tensor $\boldsymbol{\nabla}\mathbf{B}$ can be similarly written as

$$\begin{aligned} \boldsymbol{\nabla}\mathbf{B} &\equiv \left(\hat{\mathbf{e}}_{\mathrm{x}}\ \hat{\mathbf{e}}_{\mathrm{y}}\ \hat{\mathbf{b}}\right) \begin{pmatrix} \partial B_x/\partial x & \partial B_y/\partial x & \partial B_z/\partial x \\ \partial B_x/\partial y & \partial B_y/\partial y & \partial B_z/\partial y \\ \partial B_x/\partial z & \partial B_y/\partial z & \partial B_z/\partial z \end{pmatrix} \begin{pmatrix} \hat{\mathbf{e}}_{\mathrm{x}} \\ \hat{\mathbf{e}}_{\mathrm{y}} \\ \hat{\mathbf{b}} \end{pmatrix} \\ &= B_0 \left(\hat{\mathbf{e}}_{\mathrm{x}}\ \hat{\mathbf{e}}_{\mathrm{y}}\ \hat{\mathbf{b}}\right) \begin{pmatrix} \delta_x & \tau_x + \varsigma_y & \gamma_x \\ -\tau_x - \varsigma_x & \delta_y & \gamma_y \\ \kappa_x & \kappa_y & \delta_z \end{pmatrix} \begin{pmatrix} \hat{\mathbf{e}}_{\mathrm{x}} \\ \hat{\mathbf{e}}_{\mathrm{y}} \\ \hat{\mathbf{b}} \end{pmatrix}, \end{aligned} \tag{3.141}$$

in which the differential parameters of the magnetic field, including some new gradient (γ) ones which we have introduced here, are defined by:

$$\begin{array}{lll}
\delta_x \equiv \frac{1}{B}[\hat{\mathbf{e}}_{\rm x}\cdot(\hat{\mathbf{e}}_{\rm x}\cdot\boldsymbol{\nabla})\mathbf{B}], & \delta_y \equiv \frac{1}{B}[\hat{\mathbf{e}}_{\rm y}\cdot(\hat{\mathbf{e}}_{\rm y}\cdot\boldsymbol{\nabla})\mathbf{B}], & \\
\delta_z \equiv \frac{1}{B}(\hat{\mathbf{b}}\cdot\boldsymbol{\nabla})B, & & \text{divergence,} \\
\kappa_x \equiv \hat{\mathbf{e}}_{\rm x}\cdot(\hat{\mathbf{b}}\cdot\boldsymbol{\nabla})\hat{\mathbf{b}}, & \kappa_y \equiv \hat{\mathbf{e}}_{\rm y}\cdot(\hat{\mathbf{b}}\cdot\boldsymbol{\nabla})\hat{\mathbf{b}}, & \text{curvature,} \\
\tau_x \equiv -\hat{\mathbf{e}}_{\rm x}\cdot(\hat{\mathbf{b}}\cdot\boldsymbol{\nabla})\hat{\mathbf{e}}_{\rm y}, & \tau_y \equiv -\hat{\mathbf{e}}_{\rm y}\cdot(\hat{\mathbf{b}}\cdot\boldsymbol{\nabla})\hat{\mathbf{e}}_{\rm x} = -\tau_x, & \text{torsion,} \\
\varsigma_x \equiv \hat{\mathbf{e}}_{\rm x}\cdot\boldsymbol{\nabla}\times\hat{\mathbf{e}}_{\rm x}, & \varsigma_y \equiv \hat{\mathbf{e}}_{\rm y}\cdot\boldsymbol{\nabla}\times\hat{\mathbf{e}}_{\rm y}, & \text{shear,} \\
\gamma_x \equiv \hat{\mathbf{e}}_{\rm x}\cdot\boldsymbol{\nabla}\ln B, & \gamma_y \equiv \hat{\mathbf{e}}_{\rm y}\cdot\boldsymbol{\nabla}\ln B, & \\
\gamma_z \equiv \hat{\mathbf{b}}\cdot\boldsymbol{\nabla}\ln B_0 = \delta_z, & & \text{gradient } B.
\end{array} \tag{3.142}$$

Using the expression for $\boldsymbol{\nabla}\mathbf{B}$ in (3.120) yields the following Taylor series expansion for the magnetic induction field $\mathbf{B}$:

$$\begin{array}{lll}
\mathbf{B}_{\rm le} \simeq B_0\,[\,\hat{\mathbf{b}}\,(\,1 + \mathbf{x}\cdot\boldsymbol{\nabla}\ln B) & & \text{lowest order + gradient } (\boldsymbol{\nabla}B) \\
\qquad + z\,\boldsymbol{\kappa} & & \text{curvature, } \boldsymbol{\kappa} \equiv (\hat{\mathbf{b}}\cdot\boldsymbol{\nabla})\hat{\mathbf{b}} = \kappa_x\hat{\mathbf{e}}_{\rm x} + \kappa_y\hat{\mathbf{e}}_{\rm y} \\
\qquad + \tau_x\,(x\,\hat{\mathbf{e}}_{\rm y} - y\,\hat{\mathbf{e}}_{\rm x}) & & \text{torsion, } x\,\hat{\mathbf{e}}_{\rm y} - y\,\hat{\mathbf{e}}_{\rm x} = \tfrac{1}{2}\hat{\mathbf{b}}\times\boldsymbol{\nabla}(x^2+y^2) \\
\qquad + (x\,\varsigma_y\hat{\mathbf{e}}_{\rm y} - y\,\varsigma_x\hat{\mathbf{e}}_{\rm x}) & & \text{shear} \\
\qquad + (x\,\delta_x\hat{\mathbf{e}}_{\rm x} + y\,\delta_y\hat{\mathbf{e}}_{\rm y})\,] & & \text{divergence}
\end{array} \tag{3.143}$$

$$\begin{aligned}
&= B_0\,[\,\hat{\mathbf{b}}\,(\,1 + x\gamma_x + y\gamma_y + z\gamma_z) \\
&\quad + \hat{\mathbf{e}}_{\rm x}(z\kappa_x - y\tau_x - y\varsigma_x + x\delta_x) + \hat{\mathbf{e}}_{\rm y}(z\kappa_y + x\tau_x + x\varsigma_y + y\delta_y)].
\end{aligned}$$

Note that this general result simplifies to the sheared slab model (3.8) when the parameters γ_y, γ_z, κ_y ς_x, τ_x, δ_x, δ_y and δ_z all vanish, i.e., when the magnetic field does not vary in the y, z directions, and there is no shear in the x direction and no torsion of the magnetic field lines.

The solenoidal condition ($\boldsymbol{\nabla}\cdot\mathbf{B} = 0$) will be satisfied by this local expansion as long as

$$0 = \frac{1}{B}\boldsymbol{\nabla}\cdot\mathbf{B}_{\rm le} = \frac{1}{B}[\hat{\mathbf{e}}_{\rm x}\cdot(\hat{\mathbf{e}}_{\rm x}\cdot\boldsymbol{\nabla})\mathbf{B}] + \frac{1}{B}[\hat{\mathbf{e}}_{\rm y}\cdot(\hat{\mathbf{e}}_{\rm y}\cdot\boldsymbol{\nabla})\mathbf{B}] + \hat{\mathbf{b}}\cdot\boldsymbol{\nabla}\ln B = \delta_x + \delta_y + \delta_z. \tag{3.144}$$

Thus, the three diagonal components of the matrix of $\boldsymbol{\nabla}\mathbf{B}$ tensor elements are not independent; there are only 8 independent components of the $\boldsymbol{\nabla}\mathbf{B}$ tensor.

The curl of our local approximation of the magnetic induction field $\mathbf{B}$ is given by

$$\boldsymbol{\nabla}\times\mathbf{B}_{\rm le} = B_0\,[\,\hat{\mathbf{b}}\times(-\boldsymbol{\nabla}\ln B + \boldsymbol{\kappa}) + \hat{\mathbf{b}}\,(\hat{\mathbf{b}}\cdot\boldsymbol{\nabla}\times\hat{\mathbf{b}})\,], \tag{3.145}$$

in which we have made use of (3.136). As in the sheared slab model, for plasma equilibrium situations where the magnetostatic Ampere's law applies, the currents flowing in the plasma provide further constraint relations between the various local differential parameters involved in (3.145). In particular, since currents perpendicular to magnetic fields are typically small, usually $\boldsymbol{\kappa} \simeq \boldsymbol{\nabla}_\perp \ln B$

$\equiv -\hat{\mathbf{b}}\times(\hat{\mathbf{b}}\times\boldsymbol{\nabla}\ln\mathbf{B})$, i.e., the curvature vector is approximately equal to the perpendicular gradient of the magnetic field strength. Also, the parallel "shear" (parallel component of vorticity in the magnetic field $\hat{\mathbf{b}}\cdot\boldsymbol{\nabla}\times\hat{\mathbf{b}} = \mu_0\mathbf{B}\cdot\mathbf{J}/B^2$) is nonzero only if current flows along the magnetic field, i.e, $\mathbf{B}\cdot\mathbf{J}\neq 0$.

The curvature, shear and perpendicular gradient properties of a magnetic field were discussed in the context of the sheared slab model in Section 3.1. They are illustrated in Fig. 3.2 and their effects mathematically described in (3.14) and (3.24). The additional magnetic field line properties of torsion and divergence can be understood as follows.

Eliminating all but the torsion terms in (3.143), the x, y, z equations governing the trajectory of a magnetic field line deduced from (3.28) become simply

$$\frac{dx}{d\ell} = -\,y\,\tau_x, \quad \frac{dy}{d\ell} = x\,\tau_x, \quad \frac{dz}{d\ell} = 1 \implies \ell = z.$$

Dividing the second equation by the first yields

$$\frac{dy}{dx} = -\,\frac{x}{y} \qquad \Longrightarrow \qquad d\,(x^2+y^2) = 0,$$

whose solution is

$$x^2 + y^2 \;=\; x_0^2 + r_0^2 \;\equiv\; r_0^2 \;=\; \text{constant}.$$

This result can be used to reduce the equation for $dx/d\ell = dx/dz$ to one in only two variables:

$$\frac{dx}{dz} \;=\; -\,y\,\tau_x \;=\; -\,(r_0^2 - x^2)^{1/2}\tau_x \qquad \Longrightarrow \qquad \arcsin\frac{x}{r_0} \;=\; -\,z\,\tau_x + \text{constant}.$$

The equations governing a field line with torsion τ_x that passes through the point x_0, y_0 are thus given by

$$x = r_0\sin(-z\tau_x + \varphi_0), \quad y = r_0\cos(-z\tau_x + \varphi_0), \quad \varphi_0 \equiv \arctan(y_0/x_0). \tag{3.146}$$

These equations show that torsion means that as one moves along a magnetic field line it undergoes circular motion through an angle of one radian in an axial distance of $\tau_x^{-1} \equiv L_\tau$ in the plane perpendicular to the magnetic field — see Figure 3.9a. Comparing the field line trajectory equations for torsion with that derived previously for shear, (3.24), or Fig. 3.9a with 3.9b, we see that whereas torsion represents "rigid body" rotation or twisting of the field lines in the plane perpendicular to the magnetic field, shear ($\varsigma_x = 0$, $\varsigma_y \neq 0$ for Fig. 3.2b) represents differential twisting of field lines out of a plane (the x–z plane for $\varsigma_y \neq 0$). Thus, whereas the torsion terms can be removed by transforming to a rotating coordinate system, the effects of magnetic shear cannot be removed by such coordinate transformations.

To explore the divergence of magnetic field lines we eliminate all but the δ_x and δ_z terms in (3.143), and take $\delta_z = -\,\delta_x$ so as to satisfy the solenoidal condition (3.144). Then, the equations governing the magnetic field line trajectory

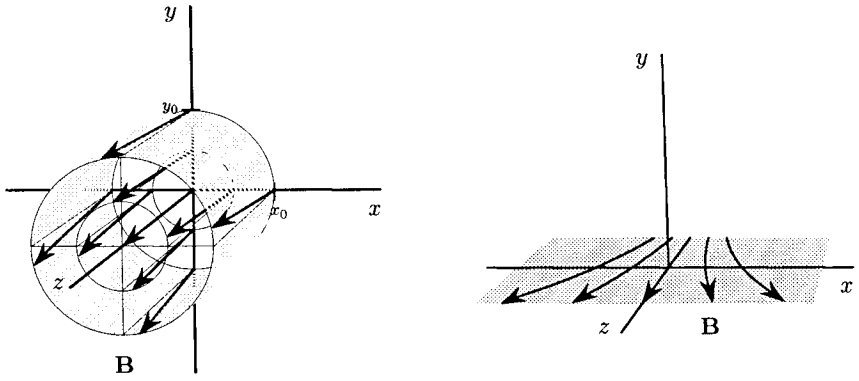

a) torsion ($\tau_x \neq 0$) b) divergence ($\delta_x = -\delta_z > 0$)

Figure 3.9: Additional magnetic field line characteristics. In each sketch the nature of magnetic field lines are indicated when only the identified coefficient(s) do not vanish.

in the x–z plane become

$$\frac{dx}{d\ell} \,=\, x\,\delta_x, \quad \frac{dz}{d\ell} \,\simeq\, 1.$$

Integrating the first equation a short distance ($z\,\delta_x << 1$) along the magnetic field line that passes through the point $\mathbf{x} = (x_0, 0, 0)$ yields

$$x(z) \,=\, x_0\, e^{\delta_x z} \,=\, x_0\, e^{-\delta_z z} \,=\, x_0 \exp\left[-\,z\,\frac{d\ln B}{dz}\right] \,\simeq\, \frac{x_0\,B(0)}{B(z)}. \qquad (3.147)$$

This result shows that the divergence ($\delta_x > 0$) in the x–z plane (cf., Fig. 3.9b) is accompanied by a decrease in the magnetic field strength [$\delta_z \equiv d\ln B/dz < 0$, $B(z) < B(0)$ for $z > 0$], as is required by the solenoidal condition $\boldsymbol{\nabla}\cdot\mathbf{B} = 0$ — see (3.2) and (3.144). The divergence scale length δ_x^{-1} (or equivalently $|\delta_z|^{-1}$) is the linear extrapolation distance along a field line over which the density of magnetic field lines would decrease (increase for $\delta_x < 0$, $\delta_z > 0$) in magnitude by a factor of two and the field lines diverge (converge) by a factor of e.

We can also develop a Taylor series expansion of the magnetic induction field $\mathbf{B}(\mathbf{x})$ about a given magnetic field line. Here, we define $\mathbf{x}_\perp = -\hat{\mathbf{b}}\times(\hat{\mathbf{b}}\times\mathbf{x})$ as the "small" vectorial distance off a given magnetic field line in the x, y plane locally perpendicular to the field line. The axial distance along the magnetic field line is parameterized by the length ℓ along it from an initial reference point. Thus,

the desired expansion is

$$\begin{aligned}\mathbf{B}_{\rm le}(\mathbf{x}_\perp,\ell) &= B_0(\ell)\,\hat{\mathbf{b}}_0(\ell) + \mathbf{x}_\perp\cdot\boldsymbol{\nabla}\mathbf{B}_0(\ell)\\ &= B_0(\ell)\,\Big(\hat{\mathbf{b}}_0(\ell)\,[\,1+\mathbf{x}_\perp\cdot\boldsymbol{\nabla}\ln B_0(\ell)\,]\\ &\quad + \tfrac{1}{2}\tau_x\hat{\mathbf{b}}_0(\ell)\times\boldsymbol{\nabla}(x^2+y^2) + [x\,\varsigma_y\hat{\mathbf{e}}_{\rm y} - y\,\varsigma_x\hat{\mathbf{e}}_{\rm x}] + [x\,\delta_x\hat{\mathbf{e}}_{\rm x} + y\,\delta_y\hat{\mathbf{e}}_{\rm y}]\Big)\end{aligned} \tag{3.148}$$

in which all quantities are now evaluated on a particular field line (i.e., at $\mathbf{x}_\perp = \mathbf{0}$), but the functional dependence on ℓ remains. Compared to the expansion about a point given in (3.143), we see that the curvature ($\boldsymbol{\kappa}$) and parallel gradient (γ_z) or divergence (δ_z) terms are missing from the expansion about a field line — because these effects are included via $\hat{\mathbf{b}}_0(\ell)$ and $B_0(\ell)$. Note also that this field line expansion for $\mathbf{B}$ satisfies the solenoidal condition $\boldsymbol{\nabla}\cdot\mathbf{B}=0$ as long as (3.144) is satisfied, and yields the result given in (3.145) for $\boldsymbol{\nabla}\times\mathbf{B}$. Since charged particles in a plasma usually move much more easily (and hence traverse much longer distances) along magnetic field lines than perpendicular to them, the expansion about a field line is usually more useful, at least conceptually, for plasma physics applications.

As discussed in Sections 3.2, 3.4–3.6, often in plasma physics there exist a set of nested magnetic flux surfaces $\psi(\mathbf{x})$ that surround nested bundles of magnetic field lines. When such surfaces exist, $\boldsymbol{\nabla}\psi$ is locally perpendicular to the magnetic field and it can be used to specify the directions of the unit vectors in the plane locally perpendicular to the magnetic field:

$$\hat{\mathbf{e}}_{\rm x} \equiv \boldsymbol{\nabla}\psi/|\boldsymbol{\nabla}\psi|, \quad \hat{\mathbf{e}}_{\rm y} \equiv \hat{\mathbf{b}}\times\boldsymbol{\nabla}\psi/|\hat{\mathbf{b}}\times\boldsymbol{\nabla}\psi| = \hat{\mathbf{b}}\times\boldsymbol{\nabla}\psi/|\boldsymbol{\nabla}\psi|. \tag{3.149}$$

For such cases it is customary to call the curvature component in the direction perpendicular to the magnetic flux surfaces (i.e., in the $\boldsymbol{\nabla}\psi$ direction) the normal curvature and the curvature component within the magnetic flux surface (i.e., in the $\hat{\mathbf{b}}\times\boldsymbol{\nabla}\psi$ direction) the geodesic curvature:

$$\begin{aligned}\kappa_x &= \kappa_\psi \equiv \boldsymbol{\kappa}\cdot\boldsymbol{\nabla}\psi/|\boldsymbol{\nabla}\psi|, && \text{normal } (\boldsymbol{\nabla}\psi) \text{ curvature},\\ \kappa_y &= \kappa_{\hat{\mathbf{b}}\times\nabla\psi} \equiv \boldsymbol{\kappa}\cdot\hat{\mathbf{b}}\times\boldsymbol{\nabla}\psi/|\boldsymbol{\nabla}\psi|, && \text{geodesic } (\hat{\mathbf{b}}\times\boldsymbol{\nabla}\psi) \text{ curvature}.\end{aligned} \tag{3.150}$$

Since this x coordinate direction is in the direction of the gradient of a scalar, the shear in the x direction vanishes: $\varsigma_x = \boldsymbol{\nabla}\psi\cdot\boldsymbol{\nabla}\times\boldsymbol{\nabla}\psi/|\boldsymbol{\nabla}\psi|^2 = 0$. However, there can still be shear in the y direction; it can be written as

$$\varsigma_y = \frac{(\hat{\mathbf{b}}\times\boldsymbol{\nabla}\psi)\cdot\boldsymbol{\nabla}\times(\hat{\mathbf{b}}\times\boldsymbol{\nabla}\psi)}{|\hat{\mathbf{b}}\times\boldsymbol{\nabla}\psi|^2}, \quad \text{shear for } \hat{\mathbf{e}}_{\rm x}\propto\boldsymbol{\nabla}\psi. \tag{3.151}$$

The torsion for this situation where magnetic flux surfaces are assumed to exist can be written as

$$\tau_x = -\frac{\boldsymbol{\nabla}\psi\cdot(\hat{\mathbf{b}}\cdot\boldsymbol{\nabla})(\hat{\mathbf{b}}\times\boldsymbol{\nabla}\psi)}{|\boldsymbol{\nabla}\psi|^2}, \quad \text{torsion for } \hat{\mathbf{e}}_{\rm x}\propto\boldsymbol{\nabla}\psi. \tag{3.152}$$

Using these relations in (**??**) along with the fact that for $\hat{\mathbf{e}}_x \propto \boldsymbol{\nabla}\psi$ we have $\varsigma_x \equiv \hat{\mathbf{e}}_x \cdot \boldsymbol{\nabla} \times \hat{\mathbf{e}}_x = (\boldsymbol{\nabla}\psi/|\boldsymbol{\nabla}\psi|) \cdot \boldsymbol{\nabla} \times (\boldsymbol{\nabla}\psi/|\boldsymbol{\nabla}\psi|) = 0$, we can write the parallel shear in the magnetic field as

$$\sigma \equiv \hat{\mathbf{b}} \cdot \boldsymbol{\nabla} \times \hat{\mathbf{b}} = \mu_0 \mathbf{B} \cdot \mathbf{J}/B^2 = \varsigma_y + 2\,\tau_x, \quad \text{parallel shear for } \hat{\mathbf{e}}_x \propto \boldsymbol{\nabla}\psi. \tag{3.153}$$

Note that this relation provides a relationship between the parallel current and the torsion and shear in the magnetic field. It is the parallel current analogy to the relationship between the curvature vector, $\boldsymbol{\nabla}_\perp \ln B$ and perpendicular current given in (3.20). Finally, the x and y field line divergence parameters can be written as

$$\delta_x = -\,\hat{\mathbf{b}} \cdot (\hat{\mathbf{e}}_x \cdot \boldsymbol{\nabla})\hat{\mathbf{e}}_x = (\hat{\mathbf{b}} \times \hat{\mathbf{e}}_x) \cdot \boldsymbol{\nabla}(|\boldsymbol{\nabla}\psi|^{-1}) \times \boldsymbol{\nabla}\psi = -\,(\hat{\mathbf{b}} \cdot \boldsymbol{\nabla}) \ln |\boldsymbol{\nabla}\psi|, \tag{3.154}$$

$$\delta_y = -\,\delta_x - \delta_z = (\hat{\mathbf{b}} \cdot \boldsymbol{\nabla}) \ln |\boldsymbol{\nabla}\psi| - (\hat{\mathbf{b}} \cdot \boldsymbol{\nabla}) \ln B, \quad \text{divergences with } \hat{\mathbf{e}}_x \propto \boldsymbol{\nabla}\psi. \tag{3.155}$$

These simplified formulas for the situation where the x coordinate is taken to be in the magnetic flux surface gradient direction are the most commonly used ones in plasma physics.

REFERENCES AND SUGGESTED READING

Plasma physics books that discuss some aspects of the structure of magnetic fields include

Bittencourt, *Fundamentals of Plasma Physics*, Chapt. 3 (1986) [**?**]

Hazeltine and Meiss, *Plasma Confinement*, Chapt. 3 (1992) [**?**]

Miyamoto, *Plasma Physics for Nuclear Fusion*, Chapt. 2 (1980) [**?**]

Schmidt, *Physics of High Temperature Plasmas* (1966,79) [**?**]

White, *Theory of Tokamak Plasmas*, Chapts. 1–2 (1989) [**?**]

Comprehensive treatments of the structure of magnetic fields for plasma physics applications are given in

Morozov and Solov'ev, "The Geometry of the Magnetic Field" in *Reviews of Plasma Physics*, M.A. Leontovich Ed., Vol.2, p.1 (1966). [**?**]

D'haeseleer, Hitchon, Callen and Shohet, *Flux Coordinates and Magnetic Field Structure* (1991) [**?**]

PROBLEMS

3.1 The magnetic field strength inside a solenoidal magnet composed of a series of circular coils can be characterized by a uniform magnetic field $\mathbf{B} = B_0 \hat{\mathbf{e}}_z$ plus a small ripple field whose magnitude on axis is given by $\delta B = \tilde{B} \sin(2\pi z/L)$ in which L is the axial distance between the magnets and $\tilde{B} << B$. Develop a sinusoidal model of the type given by (3.6) for this situation; that is, specify all the parameters of the sinusoidal model for this "bumpy cylinder" magnetic field. Sketch the behavior of the field lines inside the solenoid using (3.3). /

3.2 First, show that the magnetic field around a wire carrying a current I in the z direction is given by $\mathbf{B} = [\mu_0 I/(2\pi r)]\hat{\mathbf{e}}_\theta$, where r is the radius from the center of the wire. Next, show that the curvature vector for this magnetic field is $\boldsymbol{\kappa} = -\hat{\mathbf{e}}_r/r$ and hence that the radius of curvature of the magnetic field lines is r. Finally, show that for the simple magnetic field $\boldsymbol{\kappa} = \boldsymbol{\nabla}_\perp B$. /

3.3 Show by direct calculation starting from (3.15) that for a vacuum ($\mathbf{J} = \mathbf{0}$) magnetic field which can be represented by $\mathbf{B} = -\boldsymbol{\nabla}\Phi_M$ one obtains $\boldsymbol{\kappa} = \boldsymbol{\nabla}_\perp \ln B$, as follows from (3.20) for this situation. //

3.4 Integrate the field line equation $dx/dz = B_x/B_z$ for the sheared slab model to obtain the field line trajectory in the $y =$ constant plane. Why is the result slightly different from that in (3.14)? /

3.5 Use (3.31) to determine a potential representation for the bumpy cylinder magnetic field given in Problem 3.1 in the form of $\Phi_M = \Phi_{M0}(z) + \tilde{\Phi}_M(r,z)$. Check your result by calculating $|\mathbf{B}|$ for your model and comparing it to the desired result. //

3.6 Propose a suitable magnetic flux and a vector potential for a cylindrical model of an infinite, homogeneous magnetic field, and show that they yield the desired magnetic field. /

3.7 Calculate Clebsch α, β and ℓ coordinates for the sheared slab model as follows. First, write down three independent field line equations for dx/dz, dy/dz, and $dz/d\ell$. Integrate the first two of these equations to obtain

$$\alpha(\mathbf{x}) = B_0\left(x + x^2/2L_B - z^2/2R_C\right) = \text{constant} \quad \Longrightarrow \quad x = x(z,\alpha)$$

$$\beta(\mathbf{x}) = y - \frac{1}{L_S}\int_0^z \frac{dz'\, x(z',\alpha)}{1 + x(z',\alpha)/L_B} = \text{constant} \quad \Longrightarrow \quad y = y(z,\alpha,\beta).$$

Show that the indicated field line equations reduce to (3.14) and (3.24) near the origin. In which directions do $\boldsymbol{\nabla}\alpha$ and $\boldsymbol{\nabla}\beta$ point? Also, show that $\boldsymbol{\nabla}\alpha\times\boldsymbol{\nabla}\beta$ yields the slab model field given in (3.8). Next, integrate the third field line equation to obtain an expression for ℓ that is correct through first order. Calculate $\boldsymbol{\nabla}\ell$; in what direction does it point? Finally, calculate $\mathbf{B}\cdot\boldsymbol{\nabla}\ell$; explain why your result is (or is not) physically reasonable. //

3.8 For the sheared slab model, why is the field line equation in (3.14) different from that implied by constancy of the Ψ_z in (3.41) or the α given in the preceding problem? /

3.9 Show that the toroidal and poloidal magnetic field components given in (3.44) give the respective toroidal and poloidal magnetic fluxes. //

3.10 Show that when closed toroidal magnetic flux surfaces exist the toroidal and poloidal magnetic fluxes can be calculated from $2\pi\Psi_{\rm tor} = \int d^3x\, \boldsymbol{\nabla}\cdot\zeta\,\mathbf{B}$ and $2\pi\Psi_{\rm pol} = \int d^3x\, \boldsymbol{\nabla}\cdot\theta\,\mathbf{B}$ in which the volume integrals are taken over a closed toroidal flux surface. [Hint: A relevant volume for the toroidal surface $\Psi_{\rm tor}$ encloses a torus defined by Ψ surfaces that satisfy $\mathbf{B}\cdot\boldsymbol{\nabla}\Psi = 0$, but has a cut at a $\zeta =$ constant plane.] ///

3.11 Obtain the radial curvature κ_R from a definition like (3.13) for an axisymmetric magnetic mirror. /*

3.12 Develop a magnetic flux representation in the form $\Psi(R,\theta) = \Psi_0(R) + \tilde{\Psi}(R,Z)$ for the bumpy cylinder magnetic field given in Problem 3.1. Check your result by calculating $|\mathbf{B}|$ for your model and comparing it to the desired result. //*

3.13 Give an approximate equation for the variation of the radius of a field line in the bumpy cylinder magnetic field given in Problem 3.1 when $\tilde{B} << B_0$. /*

3.14 Write down the relevant field line equation for a dipole magnetic field. Integrate this equation to determine $r = r(\lambda)$ along a magnetic field line in terms of the radius r_0 at the equatorial plane. Substitute your result into (3.60) to obtain the variation of the magnetic field strength with λ along field lines. What is the magnetic mirror ratio to a latitude of 45^o? Finally, show that near the equatorial plane the magnetic field strength can be represented by the quadratic well model with $L_\parallel = (\sqrt{2}/3)r_0$. //*

3.15 Consider a screw pinch model situation where current only flows parallel to the magnetic field. Assume the parallel current density is given by $\mathbf{J} = J_\parallel(r)\hat{\mathbf{b}}$ with $J_\parallel(r) \geq 0$ for $0 \leq r \leq a$. What are the axial and poloidal current densities for such a situation? Develop an expression for the toroidal magnetic field strength from (3.69) for such a situation. Show that the poloidal current effect on B_z in the large aspect ratio tokamak limit where $\epsilon/q \sim 0.1 << 1$ is of order $(\epsilon/q)^2 \sim 10^{-2} << 1$. Does the flowing current produce a diamagnetic or paramagnetic effect in the region where the current $J_\parallel$ is flowing? — that is, does it decrease or increase B_z inside the plasma? Finally, give an expression for the radial variation of the total magnetic field strength for such a case. //*

3.16 Show for the screw pinch model of a large aspect ratio tokamak with $B_z(r) \simeq B_0$ which has a well-behaved current density profile near the magnetic axis (i.e., $dJ_z/dr = 0$ at $r = 0$ so that $J_z \simeq J_0 + r^2 J_0''/2$), that q increases with radius and can be approximated by $q(r) = q(0)/(1 - r^2/r_J^2)$ near the magnetic axis. What is the sign of J_0'' for a profile peaked at $r = 0$? Determine expressions for $q(0)$ and r_J in terms of J_0 and J_0''. ///*

3.17 The value of q usually decreases with radius away from the magnetic axis in a reversed field pinch. Use the combination of the two preceding models to obtain the necessary conditions on the current profile for this to occur. ///*

3.18 Consider a "box" axial current proflile given by $J_z(r) = J_0\, H(r_0 - r)$ in which $H(x)$ is the Heaviside step function defined in (**??**). Calculate and sketch the $q(r)$ profile for this current profile in a screw pinch model of a tokamak for $0 \leq r \leq a \equiv 2\, r_0$. Why does q increase as r^2 outside the current-carrying region (i.e., for $r_0 \leq r$)? /*

3.19 Determine the forms of the magnetic field curvature vector $\boldsymbol{\kappa}$, torsion vector $\boldsymbol{\tau}$ and local shear ς for the screw pinch model in terms of the magnetic field components using $\hat{\mathbf{b}} \equiv \mathbf{B}/B = (B_z\hat{\mathbf{e}}_z + B_\theta\hat{\mathbf{e}}_\theta)/B$ in the appropriate definitions of these properties of a magnetic field. Show that the results can be written as

$$\boldsymbol{\kappa} = -\frac{B_\theta^2}{rB^2}\hat{\mathbf{e}}_r, \quad \boldsymbol{\tau} = \frac{B_\theta B_z}{rB^2}\hat{\mathbf{e}}_r, \quad \varsigma = \frac{B_z}{B}\frac{d}{dr}\left(\frac{B_\theta}{B}\right) - \frac{B_\theta}{rB}\frac{d}{dr}\left(\frac{rB_z}{B}\right).$$

Also, show that these results reduce to the forms given in (3.84), (3.81) and (3.85), respectively. //*

3.20 In a reversed field pinch (RFP) the value of $q(r)$ vanishes at the reversal surface $r_{\rm rev} \neq 0$ and it might seem from (3.86) and (3.87) that the magnetic shear is undefined there. For the screw pinch model show that the magnetic shear can be written as

$$\text{shear} = \frac{1}{L_S} = -\left(\frac{r/R_0}{q^2 + r^2/R_0^2}\right)\frac{dq}{dr}.$$

What is magnetic shear length L_S where $q = 0$? Evaluate this formula for L_S at the reversal surface for a model profile $q(r) = q_0 - (q_0 - q_{\rm edge})\ r^2/a^2$ with $q_0 = 0.2$, $q_{\rm edge} = -0.1125$ for an RFP with $R_0 = 1.6$ m and $a = 0.5$ m. //*

3.21 For tokamak plasmas with noncircular cross-sections (in the ζ = constant plane) it is customary to define an effective cylindrical winding number or safety factor: $q_{\rm cyl} \equiv 2A_{\rm pol}B_{\rm tor0}/(\mu_0 R_0 I_{\rm tor})$ in which $A_{\rm pol}$ is the cross-sectional area and $I_{\rm tor}$ is the toroidal current through that area. Show that in the circular cross-section, large aspect ratio tokamak limit $q_{\rm cyl}$ reduces to the q given in (3.74). /*

3.22 Use projections of the field line definition (3.28) to obtain equations for $d\ell/dz$ and $d\ell/d\theta$ along a field line in the screw pinch model. Integrate the field line equations to determine expressions for the length of a field line in terms of the axial distance z and the poloidal angle θ traversed by the field line: $\ell = \ell(r, z)$ and $\ell = \ell(r, \theta)$. //*

3.23 Attempt to obtain a sheared slab model around a radius $r = r_0$ for the screw pinch model by expanding the screw pinch model magnetic field in (3.77) taking the slab model $\hat{\mathbf{e}}_{\rm z}$ to be in the direction of the $\hat{\mathbf{b}}$ in (3.80) evaluated at $r = r_0$. Explain why the shear parameter obtained this way is different from the $\varsigma = 1/L_S$ indicated in the sheared slab model given in (3.86). //*

3.24 Show that for the screw pinch model magnetic field

$$(\hat{\mathbf{b}}\cdot\boldsymbol{\nabla})f = \frac{1}{B}\left(\frac{B_\theta}{r}\frac{\partial f}{\partial\theta} + B_z\frac{\partial f}{\partial z}\right) = \frac{1}{h}\left(\frac{1}{R_0 q}\frac{\partial f}{\partial\theta} + \frac{\partial f}{\partial z}\right) \simeq \frac{1}{R_0 q}\left(\frac{\partial f}{\partial\theta} + q\frac{\partial f}{\partial\zeta}\right)$$

in which $f = f(\mathbf{x})$ is any differentiable scalar function of space. /*

3.25 Give the steps used in obtaining the shear for the screw pinch given in (3.85). [Hint: First show from (3.25) that $\varsigma = (\hat{\mathbf{b}}\times\hat{\mathbf{e}}_{\rm r})\cdot\boldsymbol{\nabla}\times(\hat{\mathbf{b}}\times\hat{\mathbf{e}}_{\rm r})$ using the vector identity (**??**). Then, show that $\hat{\mathbf{b}}\times\hat{\mathbf{e}}_{\rm r} = (r/h)\boldsymbol{\nabla}\theta - (r/hR_0q)\boldsymbol{\nabla}z$ and use vector identities (**??**), (**??**) and (**??**) in evaluating the shear ς.] //*

3.26 Use the magnetostatic Ampere's law and Stokes' theorem to obtain an expression for the toroidal current flowing inside of a magnetic flux suface ψ in terms of an integral of the poloidal magnetic field in the axisymmetric toroidal model. Take the large aspect ratio tokamak limit of your result and compare it to (3.68). /*

3.27 Use projections of the field line definition (3.28) to obtain equations for $d\ell/d\zeta$ and $d\ell/d\Theta$ along a field line in the axisymmetric toroidal model. Show that the ratio of these equations gives the tokamak field line equation $d\zeta = q(\psi)\, d\Theta$. Integrate the field line equations to determine general expressions for the length of a field line in terms of the toroidal and poloidal angles ζ and Θ traversed by the field line: $\ell = \ell(\psi, \zeta)$ and $\ell = \ell(\psi, \Theta)$. Show that in the large aspect ratio tokamak expansion $\ell \simeq R_0\,\zeta = R_0\, q(\psi)\,\Theta$ and indicate the order of the lowest order corrections to these results. ///*

3.28 Show that for the axisymmetric toroidal magnetic field given in (3.27)

$$\hat{\mathbf{b}}\cdot\boldsymbol{\nabla}f = \left(\frac{\mathbf{B}\cdot\boldsymbol{\nabla}\Theta}{B}\frac{\partial f}{\partial\Theta} + \frac{I}{BR^2}\frac{\partial f}{\partial\zeta}\right) = \frac{I}{BR^2 q}\left(\frac{\partial f}{\partial\Theta} + q\frac{\partial f}{\partial\zeta}\right)$$

in which $f = f(\mathbf{x})$ is any differentiable function of space. [Hint: Use chain rule rule differentiation to write $\boldsymbol{\nabla} = (\boldsymbol{\nabla}\psi)\partial/\partial\psi + (\boldsymbol{\nabla}\Theta)\partial/\partial\Theta + (\boldsymbol{\nabla}\zeta)\partial/\partial\zeta$.] Also, show that in the large aspect tokamak expansion this result reduces to the similar screw pinch limit result obtained in Problem 3.24. //*

3.29 Work out the general expression for the torsion for an axisymmetric toroidal configuration given in (3.118). [Hint: First show that for the axisymmetric toroidal magnetic field the normal torsion can be written in the form $\tau_{\mathsf{N}} = -(I/B^2|\boldsymbol{\nabla}\psi|^2)\boldsymbol{\nabla}\psi\cdot[(\boldsymbol{\nabla}\zeta\times\boldsymbol{\nabla}\psi)\cdot\boldsymbol{\nabla}(\boldsymbol{\nabla}\zeta\times\boldsymbol{\nabla}\psi)]$ using the first form of $(\hat{\mathbf{b}}\cdot\boldsymbol{\nabla})$ from the preceding problem, and (**??**). Next, show using (**??**) and (**??**) that $\tau_{\mathsf{N}} = -(I/B^2R^2)\boldsymbol{\nabla}\psi\cdot(\hat{\mathbf{e}}_{\mathrm{y}}\cdot\boldsymbol{\nabla}\hat{\mathbf{e}}_{\mathrm{y}}) = (I/B^2R^2)\boldsymbol{\nabla}\psi\cdot(\hat{\mathbf{e}}_{\mathrm{y}}\times\boldsymbol{\nabla}\times\hat{\mathbf{e}}_{\mathrm{y}})$ in which $\hat{\mathbf{e}}_{\mathrm{y}} \equiv \boldsymbol{\nabla}\zeta\times\boldsymbol{\nabla}\psi/|\boldsymbol{\nabla}\zeta\times\boldsymbol{\nabla}\psi| = (qR|\boldsymbol{\nabla}\psi|/I)[\boldsymbol{\nabla}\Theta - (\boldsymbol{\nabla}\psi)(\boldsymbol{\nabla}\Theta\cdot\boldsymbol{\nabla}\psi)/|\boldsymbol{\nabla}\psi|^2]$. Finally, work out the last form of τ_{N} using (**??**), (**??**) and (**??**).] ///*

3.30 Show that the large aspect ratio tokamak expansion of the general expression for local torsion yields the result indicated after the $\simeq$ in (3.118). //*

3.31 Work out the general expression for the magnetic shear in an axisymmetric toroidal configuration given in (3.119). [Hint: Use the form of $\mathbf{B}$ in (3.100) and work out $\mathbf{B}\times\boldsymbol{\nabla}\psi$ to a form with terms proportional to $\boldsymbol{\nabla}(q\Theta)$, $\boldsymbol{\nabla}\psi$ and $\boldsymbol{\nabla}\zeta$. Next, obtain $\boldsymbol{\nabla}\times(\mathbf{B}\times\boldsymbol{\nabla}\psi)$ using (**??**) and (**??**). Finally, work out the last form of (3.25) using the vector identity (**??**) to rearrange terms and $\boldsymbol{\nabla}\zeta\times\boldsymbol{\nabla}\psi\cdot\boldsymbol{\nabla} = \mathbf{B}\cdot\boldsymbol{\nabla} = (\mathbf{B}\cdot\boldsymbol{\nabla}\Theta)\,\partial/\partial\Theta$.] ///*

3.32 Show that the large aspect ratio tokamak expansion of the general expression for local shear yields the result indicated after the $\simeq$ in (3.119). //*